THE EFFECT OF MECHANICAL ALLOYING ON THE DEFORMATION BEHAVIOUR OF Ti-Mg ALLOYS

FINAL PROJECT

Written by

DIKO YUDAZAKI

040384003Y

S-1 INTERNATIONAL PROGRAM

ENGINEERING FACULTY

DEPARTMENT OF METALLURGY AND MATERIALS

DEPOK

JULY 2009

THE EFFECT OF MECHANICAL ALLOYING ON THE DEFORMATION BEHAVIOUR OF Ti-Mg ALLOYS

FINAL PROJECT

In fulfilment of the requirements of Research Project towards the degree of Sarjana Teknik

Written by

DIKO YUDAZAKI

040384003Y

S-1 INTERNATIONAL PROGRAM

ENGINEERING FACULTY

DEPARTMENT OF METALLURGY AND MATERIALS

DEPOK

JULY 2009

CERTIFICATION OF FINAL PROJECT REPORT

I hereby state that this project report with the title

THE EFFECT OF MECHANICAL ALLOYING ON THE DEFORMATION BEHAVIOUR OF Ti-Mg ALLOYS

I certify that the ideas, experimental works, results, analyses and conclusions set out in this final project report is entirely my own effort, except where otherwise indicated and acknowledged.

I further certify that the work is original and has not been previously submitted for assessment in University of Indonesia or other institution, except where specifically referenced.

Name **: Diko Yudazaki**

NPM **: 040384003Y**

Signature **:**

Date **:**

VALIDATION PAGE

This final report project is prepared and written by:

Name	: Diko Yudazaki
NPM	: 040384003Y
Course Program	: Metallurgy and Materials Engineering
Project Title	: The Effect of Mechanical Alloying on the Deformation Behaviour of Ti-Mg Alloys

Written and produced to complete the requirements to become Sarjana Teknik in Department of Metallurgy and Materials Engineering, Faculty of Engineering of University of Indonesia. This final project report has been approved and examined on the project presentation in Department of Metallurgy and Materials Engineering of University of Indonesia.

Depok, July 2009

Supervisor,

Dr. Ir. Bondan Tiara Sofyan, M.Si

ACKNOWLEDGEMENTS

Thanks to Allah SWT, with Allah SWT bless and guidance writer can complete this report on time. Acknowledgement is the least I can do to express the immense gratitude, reverence and sincerity I feel towards everyone who helped me in completing my work and for providing me the best experience through this journey of my graduate education. Therefore, I would like to acknowledge:

1. First and foremost, I would like to thank and acknowledge my supervisor in Monash University, Dr. Colleen Bettles, for her constant support, motivation, and guidance throughout the execution of my project. She is the person who fills in a very positive energy and attitude towards any task you wish to undertake and helps you through to the end.
2. I would like to thank my supervisor in University of Indonesia, Dr. Ir. Bondan Tiara Sofyan, M.Si, for her advice and guidance, especially during my 3 years in University of Indonesia, without her support there is no way in which I would have completed my degree in Monash University.
3. I would also like to acknowledge my beloved parents and family who have always believed in me, and for their pray and financial support during my study both in University of Indonesia and Monash University. My father and my mother, I dedicated this report and Sarjana Teknik degree for your happiness, thank you for everything.
4. I would also like to thank my best friends in International Program, Rachmat Imansyah, Dhiani Satiti, Leo Gading Mas, Haryman Manullang, Rahardian Ghazali, Satrio Prabowo, Noel Negara, Fitra Tinaz, for all your input, motivation during my project. Special thank to my lovely friend Arini Gumilang, for her advice and inspiration for the past 4 years.
5. I would like to recognize all fellow research team of Centre of Excellence (COE), Monash University, especially to Dr. Dacian Tomus and Dr. Hoi Pang NG, for their input and help during my project in Monash University.
6. I would also like to acknowledge, Mr. Rod Mackie, Mr. Daniel Curtis, Mr. Silvio Mantievichi, and Mrs. Jeanette, for their patience when trained me using apparatus and equipment for my project, and also for their advice.

7. All Materials Engineering student in Monash University, Andre Lerk, Robert Kerr, Daniel King, Thero Therence Tutu, Stuart Rundell, Siu Liang, Timothy Khoo, David Latshanky, and all other Materials Engineering students.
8. Finally, I would also like to thank every people who cannot be mentioned here one by one, but have direct influence toward my destination to become Sarjana Teknik.

Depok, July 2009

Diko Yudazaki

ABSTRACT

Name : Diko Yudazaki

Course Program : Metallurgy and Materials Engineering

Project Title : The Effect of Mechanical Alloying on the Deformation Behaviour of Ti-Mg Alloys

Mechanical alloying (MA) was used to produce Ti-*x*Mg alloys (x = 0, 2.5, 5, 7.5, 10 wt%Mg), and powders alloys of Ti-Mg were characterized by X-ray diffraction and Optical microscope. Investigation shows that the homogenous structure have not yet been obtained as milling Ti and Mg for 4 hours, but XRD traces indicated that mechanical alloying have produced Ti-Mg alloys as Mg peaks has disappeared from the traces. XRD results also showed that mechanical alloying and addition of Mg have direct effect on XRD broadening. Powder alloys were compacted using severe plastic deformation method, ECAP. Using Archimedes principle the density of Ti-Mg solid samples were measured and results shows that the density decreased as Mg content increases. Relative density on compacted powders indicates that ECAP has produced in excess of 98% density on each sample, and annealing improved the density.

Microstructure observation using SEM shows that ECAP has produced good inter-particles boundaries as well as some porosity and undissolved Mg particles can be observed. After annealing there is improvement in boundaries in samples containing Mg, but at the same time cause segregation of Mg, which indicates diffusion of Mg occurs faster during annealing at 600^0C. Mechanical properties measurement was conducted by ball indentation test method on annealed and un-annealed bulk samples, and the result were studied and analysed carefully, however, the final result of mechanical properties were not well understood and still require further and deeper investigation in the future.

Key Words:

Titanium alloys, mechanical alloying, equal channel pressing (ECAP).

TABLE OF CONTENTS

LIST OF FIGURES

LIST OF TABLES

LIST OF EQUATIONS

LIST OF ABBREVIATIONS

Ti : Titanium

Mg : Magnesium

MA : Mechanical Alloying

ECAP : Equal Channel Angular Pressing

XRD : X-ray Diffraction

FWHM : Full Width at Half Maximum

SEM : Scanning Electron Microscope

BIT : Ball Indentation Test

ASTM : American Standard for Testing and Materials

CHAPTER I
INTRODUCTION

1.1. BACKGROUND

Titanium is classified as light metallic material, and titanium is the fourth most abundant structural metal in the crust of the earth after aluminium, iron, and magnesium. Combination of properties such as excellent mechanical properties, great corrosion resistance, and high strength to weight ratio make titanium and its alloy suitable for many important applications. Then, due to its excellent properties, titanium and its alloy have found their use in many industries such as in aerospace, chemical, and automotive industry. Titanium and its alloy use in aircraft would provide significant weight saving due to its low weight [1].

Pure titanium has hexagonal closed packed (HCP) crystal structure or α phase at room temperature, and makes it strong compare to other light metal, and also titanium has high melting point at 1670°C. This high melting point becomes the strength of titanium, because it can be used for application that works at high temperature. In terms of price titanium falls to expensive metallic materials, this is because the process to extract titanium from its mineral is relatively difficult, and also the processing is expensive because needing vacuum to prevent stake out of oxygen and nitrogen [1, 2].

Alloying with another light metal such as magnesium and lithium is an interesting method to reduce the density of titanium, and in this project it has been attempted to alloy titanium with magnesium. By reducing the density of titanium, it is expected to reduce the weight of structural application. For example, when it is used in aerospace and automotive application reducing the density will effectively reduce the weight of the structure and thus saving fuel consumption. However, the problem appears as the melting point of titanium (1670°C) is much higher than magnesium (670°C), and this makes conventional alloying routes impossible to be implemented. A technique that can be used to alloy titanium and magnesium is mechanical alloying (MA) [4, 5].

The technique mentioned above is the best method to alloy these metallic materials, due to the alloying process not requiring melting the two metals as in conventional method, instead the alloying applied in solid state condition by mixing solid state powder materials.

Furthermore, the mechanical alloying method thus can be inferred as solid state process so it is possible to produce metals alloy that cannot be obtained by conventional alloying route, and also what makes it interesting is that the mechanical alloying (MA) usually applied at room temperature. To study the effect of Mg on Ti, in this project several Ti-*x*Mg compositions (x= 0, 2.5, 5, 7.5, 10 wt %) alloy were prepared, and appropriate characterization methods such as metallography, and X-ray diffraction (XRD) were performed to study the characteristics of powder alloys. It should be noted that Ti-0Mg had same milling as the others Ti-Mg alloys

Moreover, deformation behaviour of Ti-Mg alloy cannot be studied properly in the powder state, because there are only few techniques to examine the behaviour of elemental powder. To obtain proper deformation behaviour, it is necessary to compact the powder alloys into solid or bulk samples. Equal channel angular pressing (ECAP) was used to compact the powder alloys of Ti-Mg, this method is a severe plastic deformation method consolidating the powder alloys in a die normally containing an L shape or 90° die angle. So apart from investigation of powder alloys, this project will also cover the behaviour and properties of Ti-Mg alloy after being compacted into solid samples. In addition, another objective is to obtain Ti-Mg alloy in most cost effective way, which is by short mechanical alloying and ECAP to consolidate and improve homogeneity.

1.2. OBJECTIVE

The objectives of this present research are:

- To investigate a possible alloying method to produce Ti-Mg alloy.
- To investigate alloy addition effect of magnesium on titanium.
- To study the effect of Equal Channel Angular Pressing (ECAP) on the deformation behaviour of Ti-Mg alloys as well as to its microstructure.
- To investigate the effect of heat treatment temperature Ti-Mg ECAP-ed alloy.

1.3. SCOPE OF RESEARCH

The research covers the investigation and the characterization of Ti-Mg powder alloys with different level of magnesium content which prepared by mechanical alloying (MA) process. The characterization and synthesis of powder alloys involves the use of X-ray diffraction (XRD), and metallography techniques, and thus the alloy addition effect as well as mechanical alloying effect on the microstructure of this particular powder alloys can be studied.

Further investigation include the compaction of elemental powder mixtures of Ti-Mg into solid samples which achieved by using equal channel angular pressing (ECAP) mechanism. The compaction was necessary in order to determine the deformation behaviour of this alloy. Heat treatment was performed by annealing the samples at 600°C, so then can be compared with the samples, which have not been annealed. The density was measured after ECAP, microstructure observation using scanning electron microscope (SEM) is also performed, and the ball indentation test (BIT) was conducted to study the deformation behaviour of this Ti-Mg alloys.

CHAPTER II
LITERATURE REVIEW

2.1. Ti-Mg ALLOY

A reasonable explanation on why mechanical alloying becomes an effective method to alloy Ti and Mg can be referred to the Ti-Mg binary phase diagram as shown in **Figure 2.1**. The equilibrium solubility of magnesium in titanium is very low and processing of these alloys by conventional routes is not possible due to the high vapour pressure of Mg. It means that titanium and magnesium are immiscible as liquid due to a higher gap between melting point of Ti and Mg in which melting point is 1670°C and 670°C respectively. This means that boiling of magnesium will occur before reaching melting point of titanium. So this has proved why conventional alloying routes is impossible to be applied for alloying titanium and magnesium.

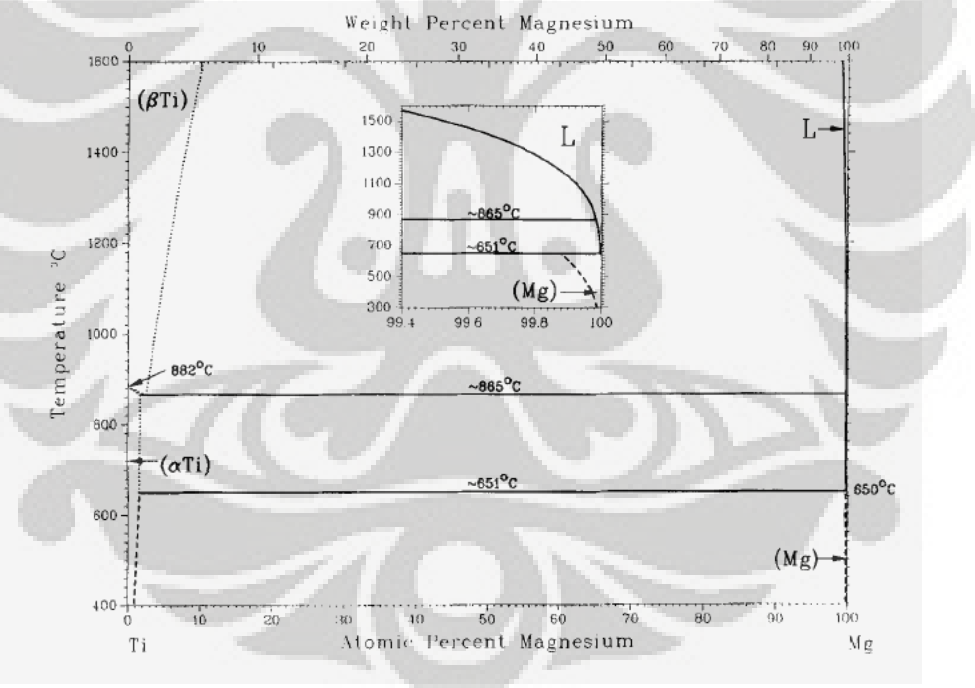

Figure 2.1: Ti-Mg binary phase diagram [3].

Titanium exists in two allotropic modifications: high-temperature (with the body-centered crystalline (bcc) lattice) and low-temperature (with the hexagonal close-packed (hcp) lattice). α-Titanium exists at temperatures below 882°C, and β-titanium at higher temperatures up to the melting point. Various elements forming solid solution with titanium are classified on the basis of their effect on the solubility of α or β phases. Elements stabilizing α phase are known as α stabilizers (Al, Ga, O, N, C), and elements stabilizing β phase are known as β stabilizers

(V, Mo, Nb, Fe, Cr, Ni, etc.). Some of the elements like Sn and Zr are neutral, as they do not stabilize either α or β phase, though they enter into solid solution with titanium [2]. However, refers to phase diagram above, there is very little mutual solubility of Mg and Ti in any phase, and no intermetallic compounds occur. Thus, the equilibrium solid phases are the low-temperature cph (αTi) and (Mg) solid solutions and the bcc solid (βTi) based on the high-temperature form of pure Ti.

The previous works have proved that it is possible to alloy Ti and Mg by using mechanical alloying method. It has been reported in previous work that mechanical alloying is the most effective way to produce Ti-Mg alloy. The method has been used to form Ti-xMg (x= 4, 9, 12, 15, 21,21, 24 at%) with variation of milling time. Characterization of alloys involved advanced technique such as XRD, and SEM. Investigation has shown that milling time and magnesium content have direct effect on the structure of Ti alloy. The longer milling time and increasing magnesium content has lead to the peaks broadening of Ti alloy XRD. Increasing magnesium content also directly affected mean diameter of mechanically alloyed powder, which is decreasing it [4].

Another work also has been reported where MA is used to produce Ti-9wt%Mg [5]. Investigation by SEM has shown that after 48 hours milling time all Mg was in solid solution, meanwhile TEM observation has shown that MA has successfully produced Ti alloy with extremely fine grains and homogeneity of Mg also has been observed.

However, despite the literature on Ti-Mg alloy produced by mechanical alloying, the effect of mechanical alloying and addition of Mg to Ti to the mechanical properties have not yet been studied. The previous research only focuses on the characterization of Ti-Mg alloys, and proving that mechanical alloying is able to produce this particular alloy combination, but in terms of measuring the mechanical properties, the research has not yet been conducted.

2.2. MECHANICAL ALLOYING

Mechanical alloying (MA) is a unique process for fabrication of several alloys and advanced materials at room temperature. Consequently, it can be used to produce alloys and compounds that are difficult or impossible to be obtained by conventional melting and casting techniques. It is a powder processing technique, which allows production of macroscopically homogeneous materials starting from various powder mixtures, and it is

being referred to as mechanical alloying because the process generally involves materials transfer during milling and causes the mixtures to alloy. Originally developed to produce oxide-dispersion-strengthened (ODS) nickel-and iron-base superalloys for application in the aerospace industry, MA has now been shown to be capable of synthesizing a variety of equilibrium and non-equilibrium alloy phases starting from blended elemental or prealloyed powders [6].

In general, the mechanism of MA can be divided into three stages which are early, intermediate, and finish stage. In early stage normally produce some flattened structure and some original size particles may remain at this stage. With continued milling, the cold welding and fracturing event continue to take place leading to microstructural refinement. At this intermediate stage the amount of cold working increases significantly, thus make the number of crystal defects (dislocations, vacancies) and number of grain boundaries increase with time. During mechanical alloying, collision that comes from the ball-ball, ball-powder, and ball-wall has made temperature of powder increases and this increasing temperature facilitates diffusion. Alloy formation occurs due to the combined effect of all these factors. Uniformity and particles refinement also occurs at this intermediate stage. Then, the final stage is a steady state stage, meaning that it is a maximum stage that can be approached in MA process, and further processing after this stage will not provide any better results [6, 7].

The actual process of MA starts with mixing of the powders in the right proportion and loading the powder mixture into the mill along with the grinding medium (generally steel balls). This mix is then milled for the desired length of time until a steady state is reached when the composition of every powder particle is the same as the proportion of the elements in the starting powder mix. During high-energy milling, powder particles are repeatedly flattened, cold welded, fractured, and rewelded. The processes of cold welding and fracturing, as well as their kinetics and predominance at any stage, depend mostly on the deformation characteristics of the starting powders. For example, the initial impact from the grinding ball to ductile powder materials cause the ductile powder to flatten and work harden, while impact to brittle intermetallic powders make the particles get fractured and refined in size, these different tendencies are shown schematically on **Figure 2.2**. Therefore, the important parameters of the MA process are the raw materials, the mill, and process variables.

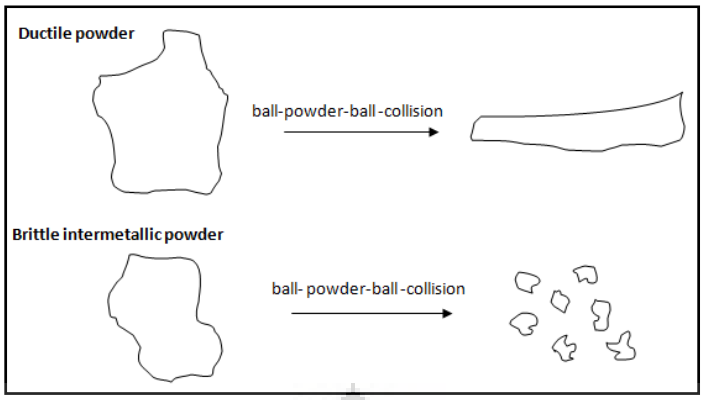

Figure 2.2: Deformation characteristics of representative constituents of starting powder in MA.

The raw materials used for MA are widely available commercially pure powders that have particles sizes in the range of 1-200μm. However, the powder particles size is not very critical, except that it should be smaller than the grinding ball size. This is because the powder particle size decreases exponentially with time and reaches a small size of a few microns only after few minutes of milling. The raw powders fall into the broad categories of pure metals, master alloys, prealloyed powders, and refractory compound. In the early days of MA, the powder charge consisted of at least 15 vol% of ductile compressibly deformable metal powder to act as host or a binder. However, in recent years, mixtures of fully brittle materials have been milled successfully resulting in alloy formation. Thus, the requirement of having a ductile metal powder during milling is no longer necessary. Accordingly, ductile-ductile, ductile-brittle, and brittle-brittle powder mixtures are milled to produce novel alloys [6, 7]. In relate to this project, Ti-Mg alloys can be classified as ductile-brittle system, and further discussion about this matter will be discussed later on this report.

Different types of high-energy milling equipment are used to produce mechanical alloyed powders. They differ in their capacity, efficiency of milling and additional arrangements for cooling, heating, etc. The different mills types available for MA are planetary ball mills, attritor mills, and SPEX shaker mills. The most common mill used for laboratory investigation and for alloy screening purposes is SPEX shaker mill. This mill is capable to mill about 10-20gr of the powder at a time. The mill has one vial, containing the sample and the grinding balls, secured in the clamp and swung energetically back and forth several thousand times a minute. The back-and-forth shaking motion is combined with lateral movements of the ends of the vial. With each swing of the vial, the ball impact against the sample at the end of the vial, both milling and alloying the powders [6, 7].

As mentioned above, the mechanical alloying product is also influenced by the processing variables. The processing variables are such as type of mill, milling container, milling speed, milling atmosphere, milling time, process control agent, grinding medium, and milling temperature. There are various types of mill for conducting MA, but a suitable mill should be chosen by considering the objective performing MA, and normally SPEX shaker mill is used for alloy screening purposes. Milling container should be considered wisely due to incorrect type of milling container material could contaminate the powders during MA. Grinding medium also should be considered carefully in order to prevent the grinding balls to contaminate the powders and thus interfere with the final structure after MA. Milling time is the most important variable, and normally the time is chosen as to achieve a steady state between the fracturing and cold welding of the powder particles. Longer milling time may be used to produce nanostructure materials, but it should be noted that the level of contamination increases and some undesirable phases might form if the powder is milled for longer times than required. Impact energy can be increased by changing the ball-to-powder-ratio, and as the impact energy level increases better uniform particles size distribution might be achieved as well as better homogeneity structure could also be achieved by changing this particular variable. Process control agents (e.g. steric acid) are normally added to prevent agglomeration of powder particles during MA [7].

2.3. EQUAL CHANNEL ANGULAR PRESSING (ECAP)

In many textbooks, the method of Equal Channel Angular Pressing (ECAP) is sometime also referred to as Equal Channel Angular Extrusion (ECAE). The process developed originally by scientists in the former Soviet Union, two decades ago [8]. In general ECAP is a processing method in which a metal is subjected to an intense plastic straining through simple shear without any corresponding change in the cross sectional dimensions of sample. The process itself is usually performed in a die containing various angles between the entry and exit channels, but the most common die used has a 90^0 angle shape. Compare to other severe plastic deformation process, ECAP offers convenient procedure for obtaining ultrafine grain materials, in which simple pressing of the metallic material through specially designed channel dies occurs without any substantial change in geometries. The principle of the ECAP process is shown in **Figure 2.3**.

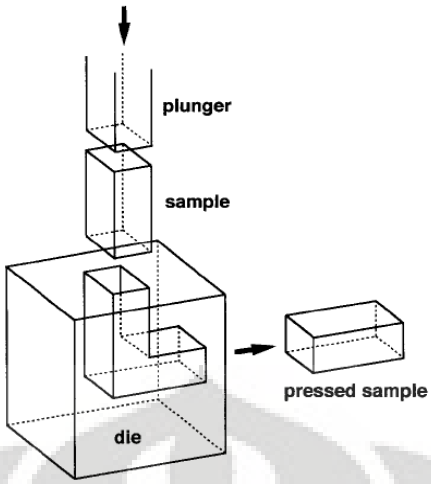

Figure 2.3: ECAP Process Principle [6].

In the ECAP process, critical variables include the die angle, temperature, number of passes through the die, and whether or not the workpiece is rotated between passes. This procedure offers several advantages over powder processing, including reduced levels of contamination, full density, and the elimination of the consolidation step.

Some previous works have attempted to consolidate powder element into bulk samples through ECAP mechanism. Firstly, it has been reported that ECAP method was used to consolidate Magnesium and Magnesium alloys powder, and the objective was to obtain good inter-particle bonding strength via ECAP, and show that ECAP could be used to achieve high relative density. This paper also demonstrates the effect of powder morphology to the final products, as well as the effects of strain rate, process temperature, and hydrostatic pressure on the quality of the billet. Then it was reported that for Magnesium powder materials the suitable ECAP back pressure was 175MPa, and ECAP should be done at temperature not higher than 150^0C [9]. Secondly, another work has also been reported, and this time ECAP was used to compact Ti−6Al−4V powder, and was performed at low compaction temperature (≤400 °C) with ≥175MPa back pressure. Then the outcome of the researched revealed that the relative density of compacts produced by ECAP at 400°C increased from 96.8 to 98.6% with increase in applied back pressure from 20−480MPa, while Vickers hardness increased from 360 to 412HV [10].

CHAPTER III

EXPERIMENTAL METHODS

3.1 FLOWCHART OF PROJECT

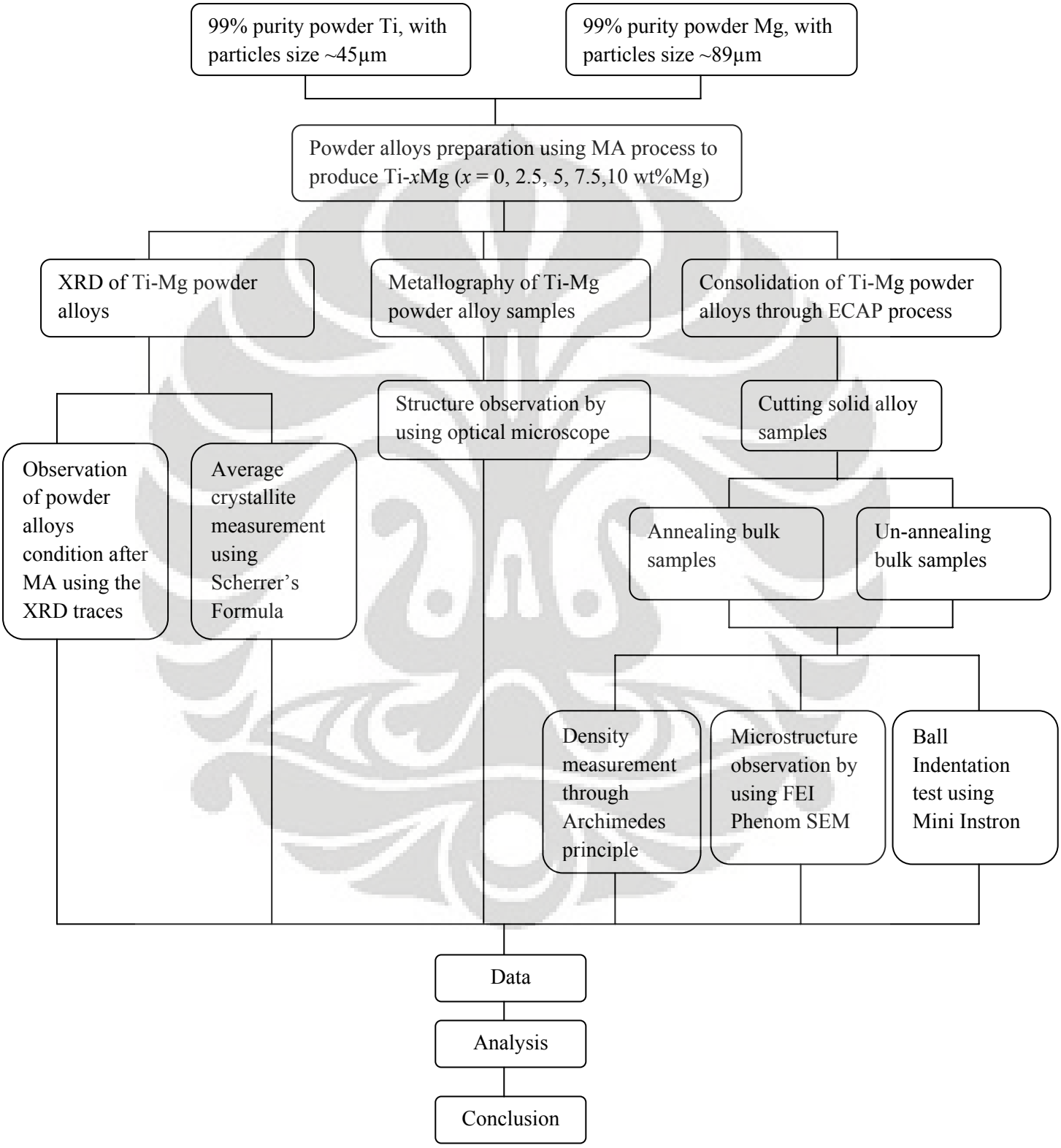

Figure 3.1: The flowchart of project.

3.2 MATERIALS AND EQUIPMENTS

3.2.1 Materials

- Commercially 99% purity Ti powder with particles size ~45μm
- Commercially 99% purity Mg powder with particles size ~89μm
- Steric acid
- Epoxy resin along with its epopix hardened
- SiC papers
- Polisher clothing
- Diamond paste for polishing
- Silica polisher clothing
- Colloidal silica suspension
- Kroll's reagent etchant (5% HNO_3, 10%HF, and 85% H_2O)
- Tetracholoroetyhlene liquid

3.2.2 Equipments

The equipments that were used during research are as followed:

1. Argon gloves box in Department of Materials Engineering, Monash University. The gloves box was used to load powder mixture of Ti-Mg into the vial, and unload the powder alloys from the vial.
2. Vial or container and grinding ball that was used for mechanical alloying process.
3. SPEX 8000 shaker mill used to perform mechanical alloying.
4. Philips X-ray diffractometer with Cu Kα radiation, and V= 40kV and i= 25mA was used.
5. Specially designed ECAP unit equipment, with backpressure applied.
6. Optical microscope Olympus BX60M that is supported Olympus camera, and a unit of computer for storing the images data.
7. Buehler low speed cutting saw.
8. Grinding machine.
9. Polishing machine, 3 micron and 1 micron.
10. Furnace for heat treatment.
11. FEI phenom touch screen SEM equipment.
12. Mini instron 5848 with the ball indenter installed and supported by computer to storage the data. Ball Indentation test was performed using this equipment.

3.3 SAMPLE PREPARATION

3.3.1 Mechanical Alloying

The mixed powders and grinding media were loaded into the vial (**Figure 3.2**) inside the argon gloves box (**Figure 3.3**), and mixing powders were mechanical alloyed in a SPEX-8000 shaker mill (**Figure 3.4**) for 4 hours with ball-to-powder ratio 10:1. In order to avoid the agglomeration of powder, it was necessary to add control agent, steric acid, before milling, and it was added along with powder mixtures at 0.75wt%. The powder alloys prepared were Ti-0, 2.5, 5, 7.5, and 10 wt% Mg.

Figure 3.2: Vial and grinding balls for mechanical alloying.

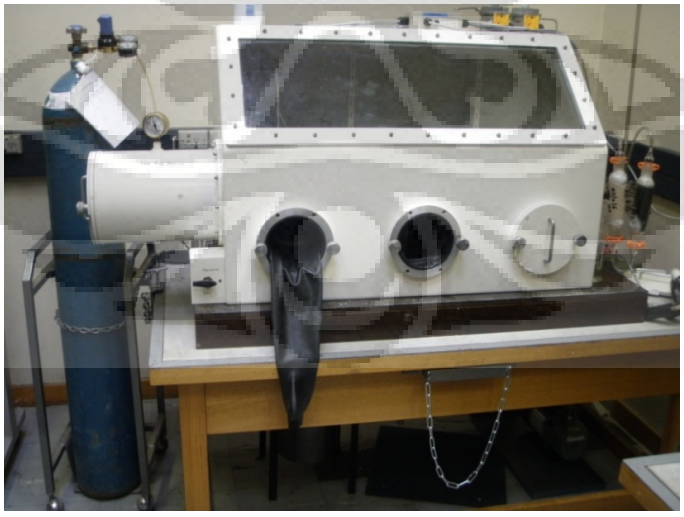

Figure 3.3: Argon gloves box.

Figure 3.4: SPEX 8000 shaker mill.

3.3.2 Equal Channel Angular Pressing (ECAP)

Powders are not practical form for most mechanical testing methods, it is thus desirable to consolidate into the bulk samples, and it was obtained by equal channel angular (ECA) processing. A single pass ECAP at 400°C with back pressure 175MPa and cross head speed instron 30mm/min was used. One unit of special designed ECAP equipment is shown in **Figure 3.5**.

Figure 3.5: ECAP unit equipment.

The vertical entry channel is 75mm in length and made a 90° angle with the horizontal exit channel. The diameter of the channels is 10 mm. The powder was poured directly into the vertical entry channel of the cold die and during pouring the backpressure punch was positioned deep within the exit channel to contain powder within the vertical channel **(Figure 3.6).**

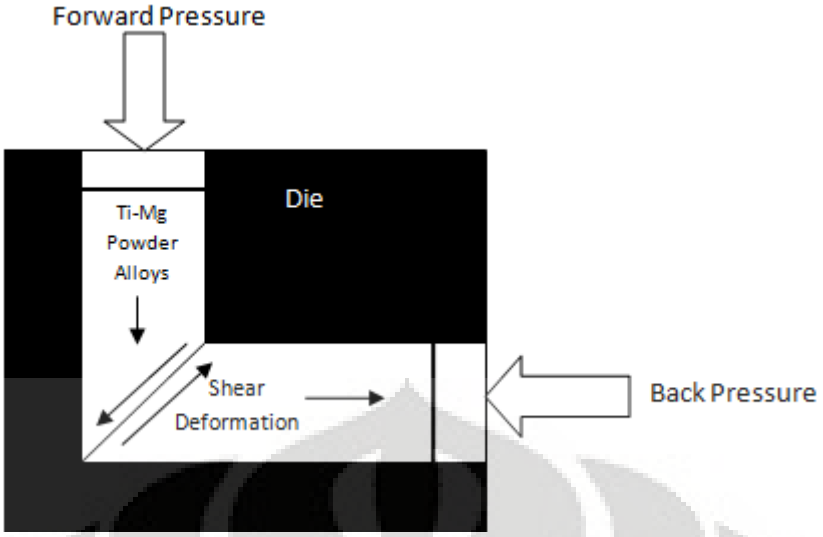

Figure 3.6: ECAP schematic process representation.

3.3.3 Cutting ECAP Samples

The solid sample obtained after ECAP is shown in **Figure 3.7 (a)**. Each bulk samples were cut into 3 parts as shown schematically in **Figure 3.7 (b)**, the bulk samples were cut using buehler low speed diamond saw (**Figure 3.8**). The cutting direction performed parallel to the shear deformation direction in ECAP. However, later it is only second part is used for density measurement, heat treatment, ball indentation test, and observation using SEM purposes. This is because sections 1 and 3 do not undergo the shear deformation. Therefore, in this case these sections are not investigated, due to the need of shear to achieve high density.

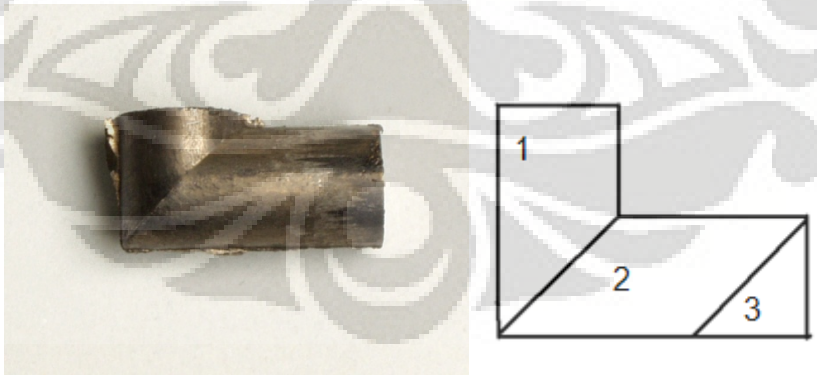

Figure 3.7: (a) ECAP sample; (b) Cutting ECAP samples into 3 parts

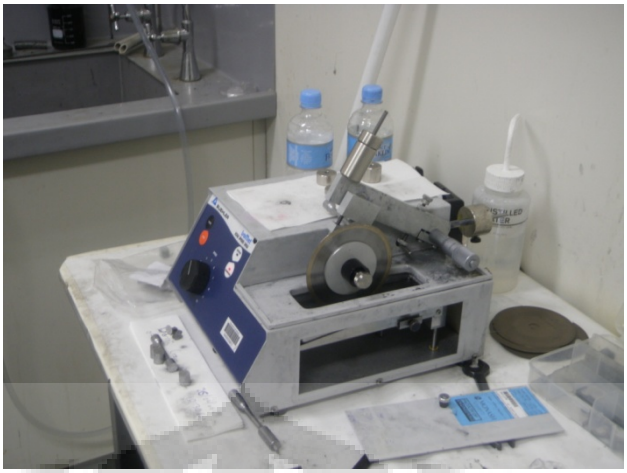

Figure 3.8: Buehler low speed saw with diamond cutting saw.

The second section mentioned before was then divided into 2 parts; the two sections were used for annealing and un-annealing purpose respectively.

3.3.4 Heat Treatment

Heat treatment that is by annealing the ECAP part mentioned above was then performed. The annealing was carried out by encapsulating the bulk samples of Ti-xMg (x = 0, 2.5, 5, 7.5, 10 wt%Mg) inside the quartz tube under argon atmosphere condition. The annealing was performed in a furnace at 600°C for 1 week. The furnace apparatus that was used is shown in **Figure 3.9**. Encapsulation of samples is significant in order to avoid oxidation of samples during annealing, and the objective of annealing is to release strain and internal stress after compaction of powder into bulk samples, and encourage diffusion to ensure the excellent interparticle bonding is achieved.

Figure 3.9: Furnace apparatus.

3.3.5 Metallography

The metallography technique method were performed on initial powder Ti and Mg, Ti-*x*Mg (x = 0, 2.5, 5, 7.5, 10 wt%Mg) powder alloys, and ECAP solid samples.

A. Powder samples

- The initial powder of Ti and Mg as well as Ti-Mg powder alloys were mounted inside epoxy resin, so that they can be observed under optical microscope.
- Grinding was conducted on SiC papers with the support of grinding apparatus with rotating disk in which the rotation speed of the disk can be controlled (**Figure 3.10**). The SiC papers used are starting from 800, 1200, and 2400.
- Polishing were conducted in 3 orders, first using polishing cloth which supported by 3 micron diamond paste, second using polishing cloth which supported by 1 micron diamond paste, and last polished by using silica paper which supported by colloidal silica suspension. The purpose of polishing is for eliminating defect, course scratch as the result of grinding processes. The polisher machine which was used is given in **Figure 3.11**.
- Etching was done by using Kroll's reagent etchant. The objective is to make the grain and microstructure of the samples become visible.

B. ECAP solid samples

- The samples were grinded with the used of SiC papers of 320, 500, 800, 1200, and 2400 grit sizes. The grinding objective is to flatten the surface of the ECAP samples that was cut by low speed diamond saw.
- The samples were polished using silica polisher cloth, and colloidal silica suspension was also used during polishing.

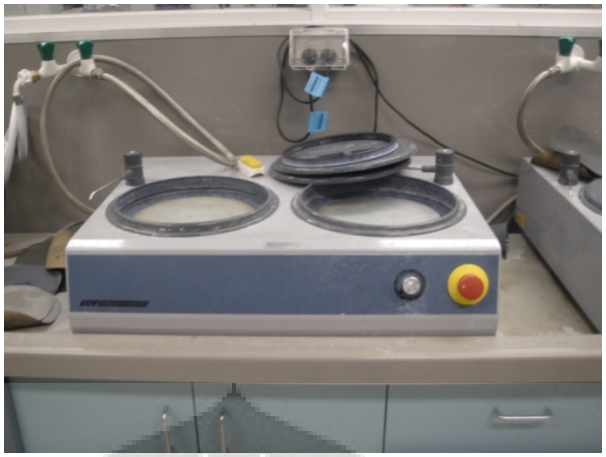

Figure 3.10: Grinding apparatus with two rotating disk and rotation speed control.

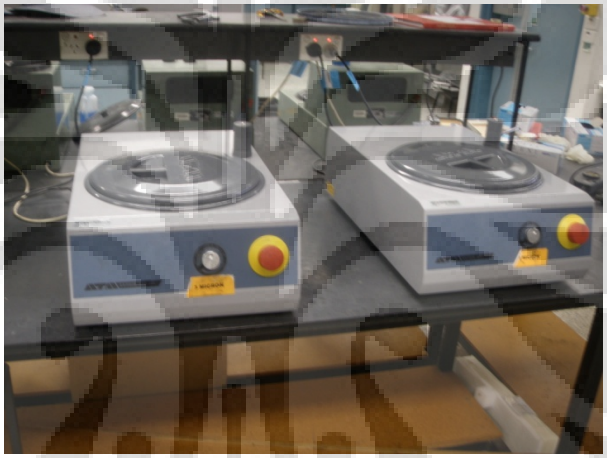

Figure 3.11: Polisher machine of 3 and 1 micron.

3.4 CHARACTERIZATION AND TESTING

The characterization and testing were performed on the powder samples and the bulk samples of Ti-Mg alloys. The methods used to characterize powder samples include the use of Optical Microscope, and X-ray diffractometer (XRD). Meanwhile, density measurement of bulk samples was conducted by using Archimedes principle, and to determine mechanical properties of the bulk samples of Ti-Mg alloys, the ball indentation test (BIT) method was used. In addition, microstructure observation of bulk samples conducted by using FEI Phenom SEM.

3.4.1 Powder Samples

A. Optical Microscope

This equipment was used to observe the morphology of powder samples. There are two magnifications that were used which is 20 and 50 times magnification, and the images

were recorded by using Olympus camera, **Figure 3.12** showing the optical microscope equipment.

Figure 3.12: Olympus BX60M Optical Microscope

B. X-ray Diffraction (XRD)

X-Ray diffraction (XRD) was then performed on each powder alloys, and the purpose of this technique is to ensure that the process of Mechanical Alloying has been successful in alloying Ti and Mg powder together. A Philips X-ray diffractometer was used with Cu Kα radiation and V=40kV and i=25mA, and the XRD was performed with 2theta range from 20° to 80°. Additionally, another useful method that can be used on XRD is determination of average crystal size using Scherrer's Formula as given in **Equation 3.1**.

$$D_v = \frac{k\lambda}{\beta \cos \vartheta} \quad \text{..... (3.1)}$$

D is average crystallite size, λ is the wave length of the X-ray radiation, k is Scherrer's constant 0.87-1, θ is the 2theta degree angle of the peaks chosen to determine β, and β is the corrected peak width defined by full width at half maximum (FWHM).

$$\beta^2 = \beta_{obs}^2 - \beta_{ins}^2 \quad \text{..... (3.2)}$$

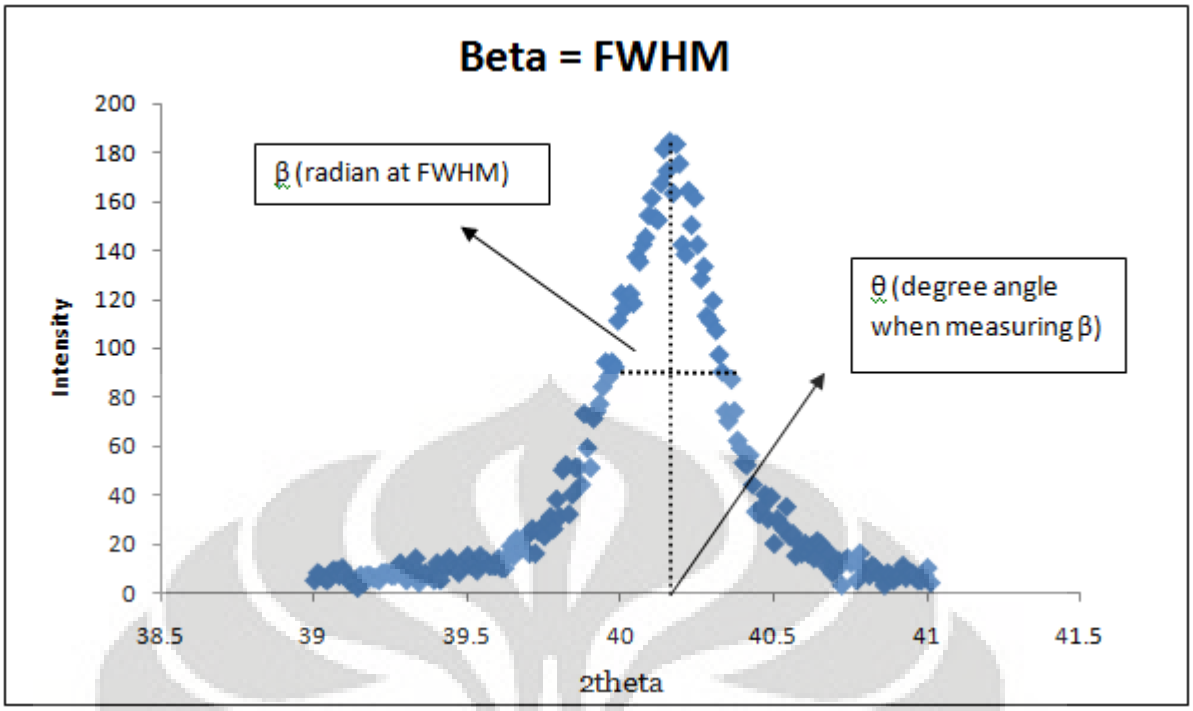

Figure 3.13: FWHM determination technique.

To obtain β **Equation 3.2** should be used, assuming that the peaks have Gaussian shape. Actually, the β value is the radian of broadening peak minus the radian of un-broadening peak at full width half maximum of peak where β_{obs} is broadening peak while β_{ins} is un-broadening peak. Then, the average crystallite size were measured by using three major peaks in Ti XRD spectra results which are at 35^0, 38^0, and 40^0 2theta degree angle, or equates to [10-10], [0002], and [10-11] planes.

3.4.2 Bulk/ECAP Samples

A. Density Measurement

The density measurement was conducted on annealed and un-annealed samples. The density of both bulk samples condition was defined by Archimedes' method (ASTM, B311-93) using tetracholoroethylene, with a density of 1.62 g cm^{-3}, as the immersion liquid. Then, the density was calculated using **Equation 3.3**.

$$\rho = \frac{W_{air}}{(W_{air} - W_{liq}) / \rho_{liq}} \quad \text{..... (3.3)}$$

B. Scanning Electron Microscope (SEM)

Scanning Electron Microscope (SEM) was then used to investigate the morphology or the microstructure obtained for both annealed and un-annealed samples. The SEM apparatus was Phenom SEM; it is a new invented SEM device which is simpler than the usual SEM device (**Figure 3.14**). There are two methods that can be applied which are backscattered (atomic contrast) and topography method, and both methods were used to investigate the morphology of both annealed and un-annealed samples.

Figure 3.14: FEI Phenom SEM device.

C. Ball Indentation Test (BIT)

To measure the mechanical properties of samples, ball indentation method was used. The method was performed using Mini-Instron device, and supported by computer to store the data obtained during test. Ball indentation test was performed on annealed and un-annealed samples, and it was performed with 8 repeated loading and unloading cycles of a sample with a Rockwell indenter (WC ball) which has spherical shape and diameter 1.57mm. The initial load was 100N and incrementing the load by 100N in each successive cycle. The indentation were performed twice for each samples, and the final results is the average of two times indentation.

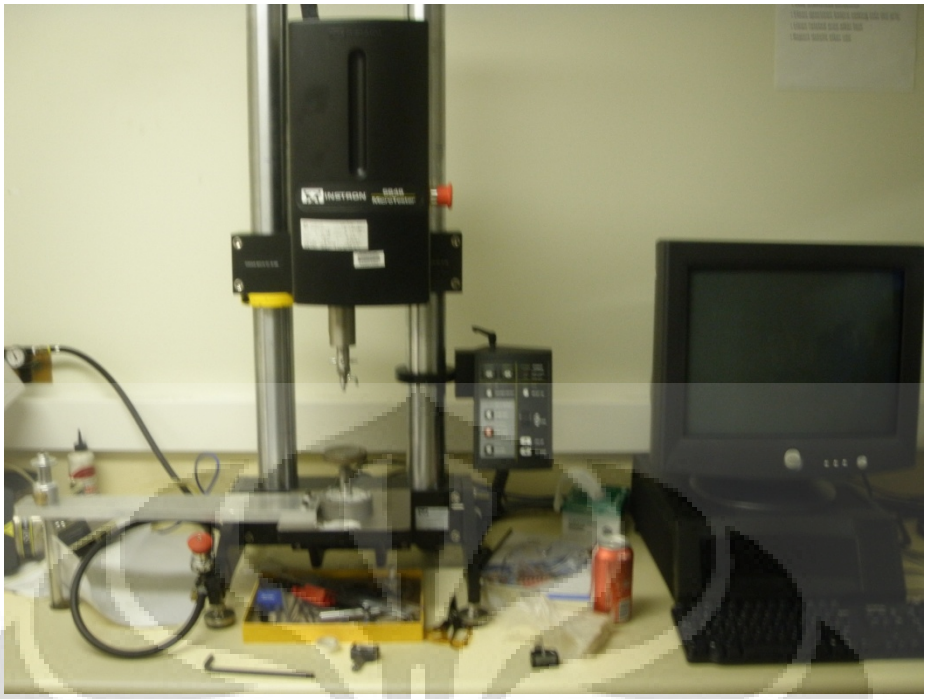

Figure 3.15: Mini Instron 5848 with a Rockwell ball indenter for ball indentation test.

CHAPTER IV
RESULTS AND DISCUSSION

4.1 POWDER SAMPLES

4.1.1 Powder Images

Figure 4.1 and 4.2 are representing the powder of titanium and magnesium respectively, and the images were taken using two different magnifications which is 20 and 50 times magnification. In **Figure 4.1** it seen that Ti powders have irregular structure, while from **Figure 4.2** shows that Mg powders have round or spherical structure. These powder have different shape due to they were produced by different method, Ti powder is produced by an embrittling method named as hydrogenation-dehydrogenation and the particles are fine chips, while Mg powder produced by gas atomisation method in which a molten of Mg is sprayed into a vacuum chamber.

Figure 4.2 also showing grain boundaries of Mg powders with the grain size ~ 25μm, and these equiaxed grains become visible after etching the Mg powders. In contrast, grain boundaries in initial Ti powder cannot be observed.

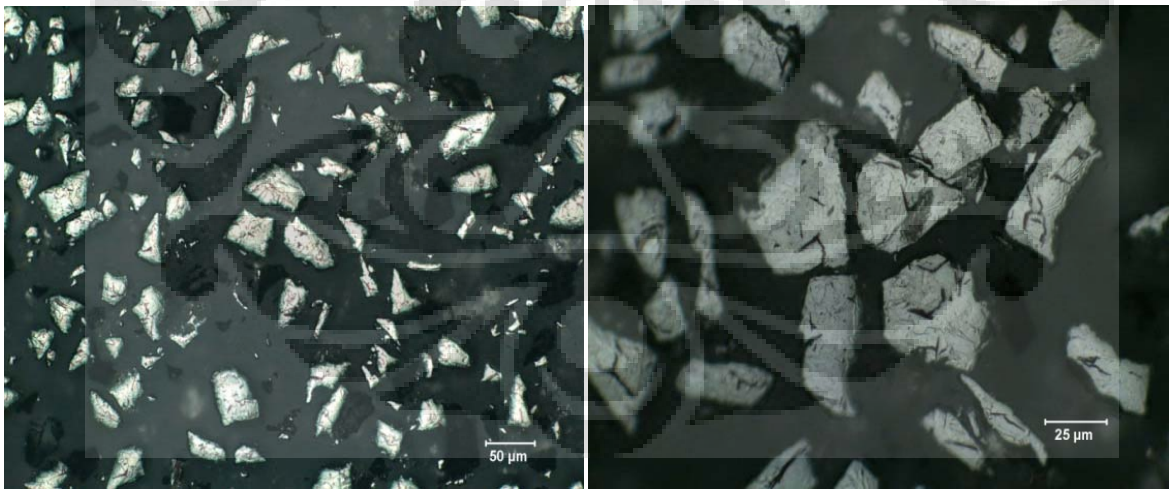

Figure 4.1: (a) &(b) the microstructure of initial Ti powder at different magnification.

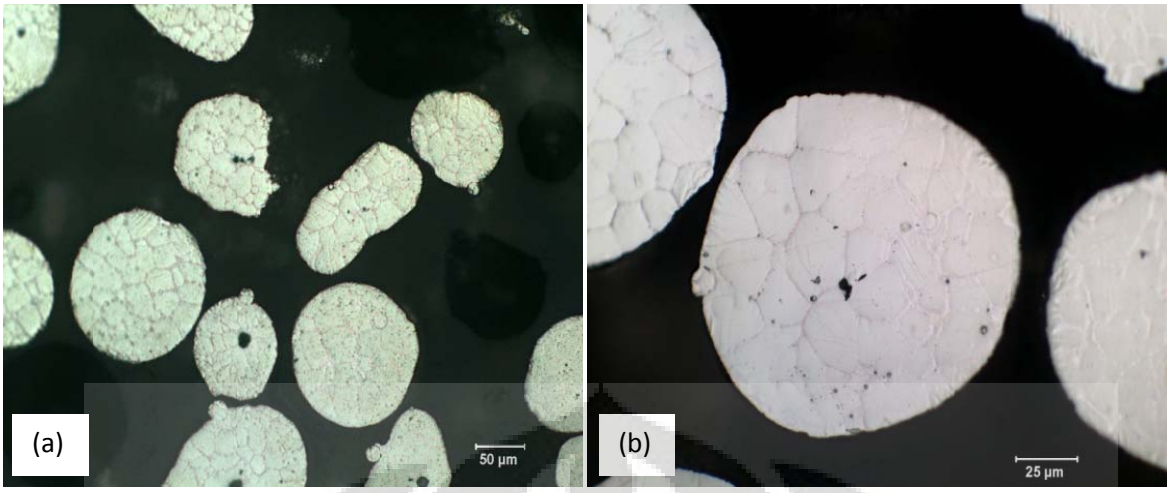

Figure 4.2: (a) & (b) the microstructure of initial Mg powder at different magnification.

Figure 4.3 to 4.6 are representing the images of Ti-xMg (x = 2.5, 5, 7.5, 10) powder alloys. There are some large and small particles which can be observed from each composition. Two regions can also be identified on each image, first is dark region (A) and second is shiny region (B) as shown on **Figure 4.3 (b)**. These two regions are representing Ti and Ti-Mg areas, and it appears that Mg not uniformly distributed in Ti, and gives indication that mechanical alloying for 4 hours have not yet produced homogenous structure. In addition, these images show that as Magnesium content increases from 2.5 to 10wt%, more Mg are in solid solution. From all compositions, only 10wt% Mg is close to homogenous structure, this could be due to it contains more Mg than the others.

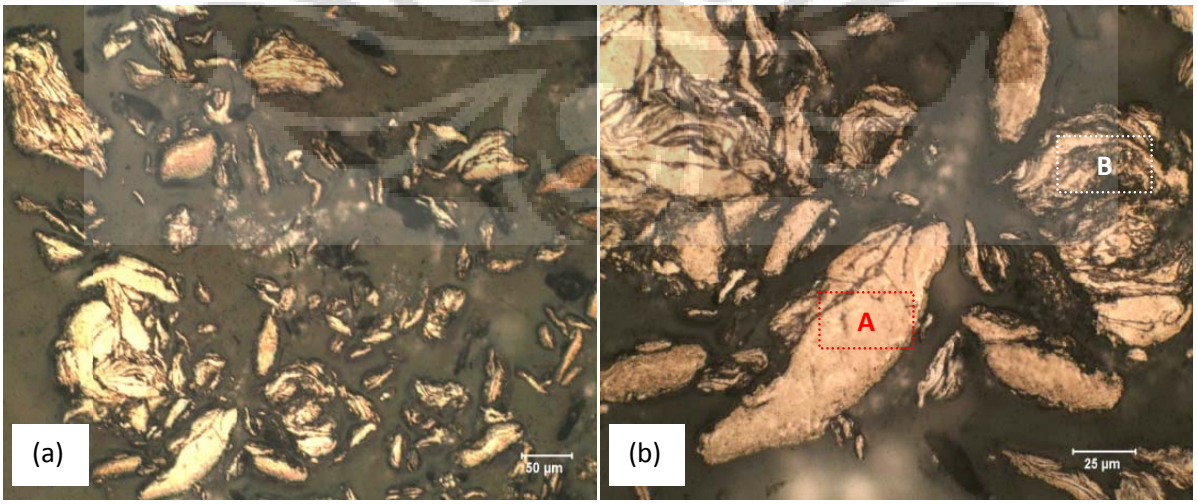

Figure 4.3: (a) & (b) microstructure of Ti-2.5Mg powder alloy with two regions appears; shinny region marked (A) is Ti and dark region marked (B) is Ti-Mg.

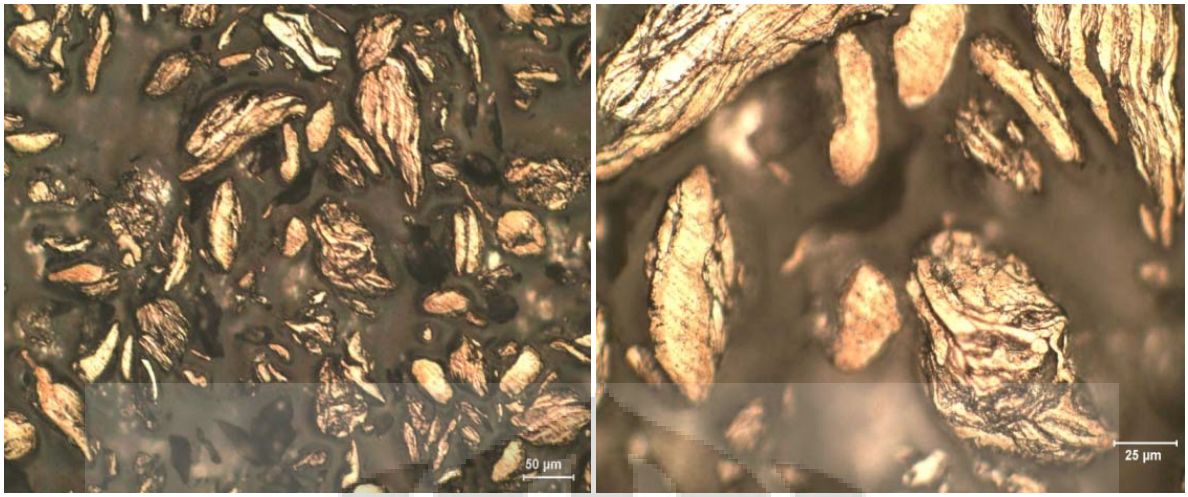

Figure 4.4: (a) & (b) microstructure of Ti-5Mg powder alloy with two regions appears.

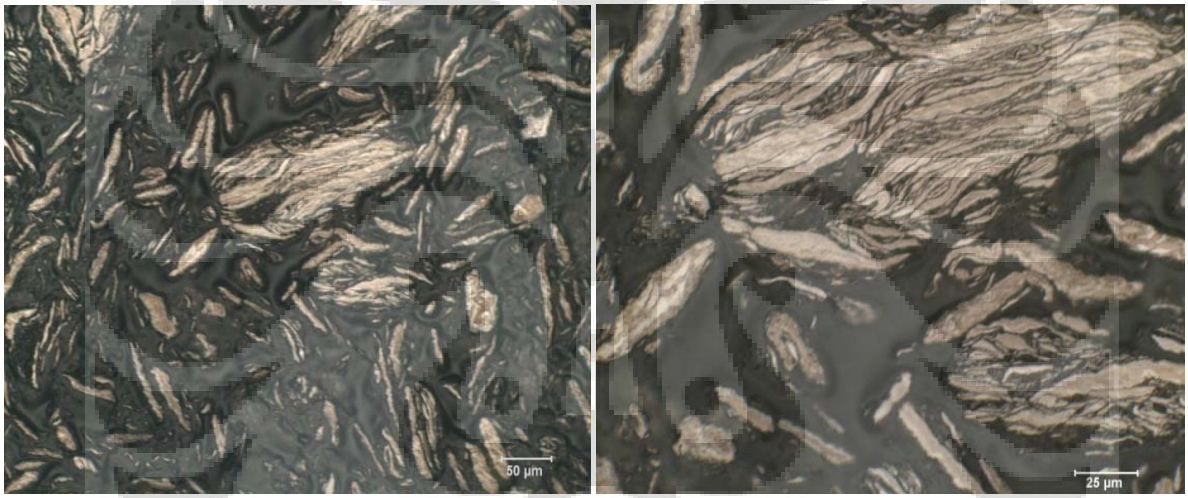

Figure 4.5: (a) & (b) microstructure of Ti-7.5Mg powder alloy with two regions appears.

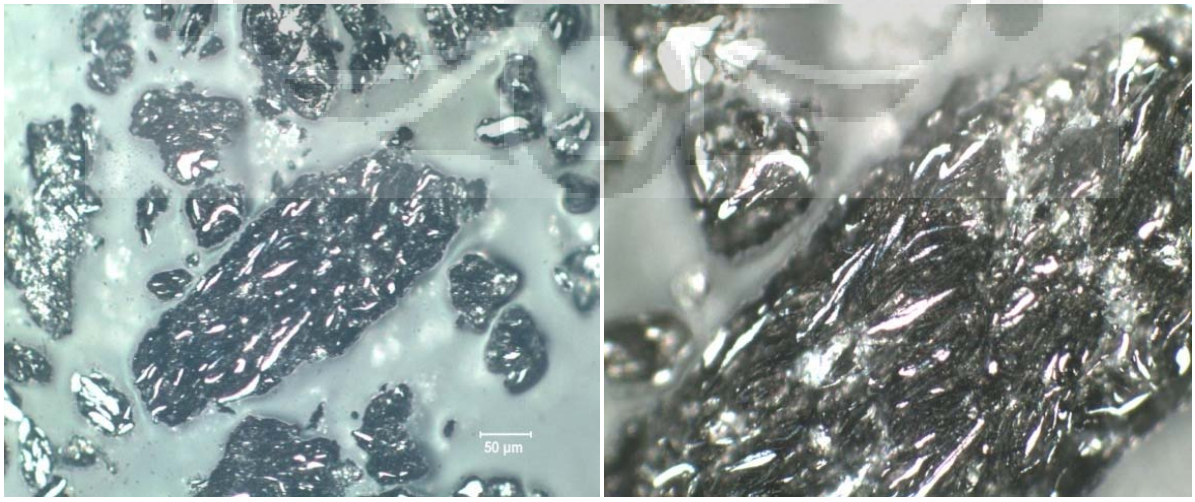

Figure 4.6: (a) & (b) microstructure of Ti-10 Mg powder alloy with two regions appears.

The mechanical alloying process has successfully produced Ti-*x*Mg (x = 0, 2.5, 5, 7.5, and 10 wt%) powder alloys. Some large particles still appear on every composition which suggests that the uniform particle size distribution cannot be completely obtained by 4hours mechanical alloying. However, different sizes of particles are actually desirable for compaction by ECAP, because to obtain better packing density it is desirable to have various particles size and shape. Packing density is the density before any load is applied during compaction or the initial density when first pouring powder alloys into ECAP die. So by having different particle size and shape, it is expected that smaller particles will close the hole in between bigger particles, and thus produce dense bulk samples after compaction. In addition, images of powders of Ti-Mg have indicating that mechanical alloying leads to both particle refinement and agglomeration of fine particles.

As have been mentioned in literature review, Ti-Mg powder alloy produced by mechanical alloying is classified as ductile-brittle system. In this particular system, the microstructure evolution is depending on the characteristic of each constituent element. In early stage of mechanical alloying, the ductile particles get flattened by the ball-powder-ball collisions, while the brittle intermetallic particles get fragmented. These fragmented brittle particles tend to become occluded by ductile constituents and trapped in the ductile particles. The brittle particles of Mg is closely spacing along the boundaries of Ti particles. With further milling the powder particles get work hardened and refined, while the insoluble brittle particles of Mg get uniformly dispersed in the Ti matrix.

Moreover, the actual process of mechanical alloying of Mg in Ti could be explained in the following ways. Mechanical alloying is a heavy deformation process, and during mechanical alloying grain boundaries and others defects such as vacancies and dislocation formed in the Ti powders, then the Mg collects in the grain boundaries of the Ti, and with further impact from milling media the Mg migrates into the interior of Ti grains.

4.1.2 X-ray Diffraction (XRD)

X-ray diffraction spectra for Ti-Mg alloys along with XRD spectra of initial powder Ti and Mg are provided in **Figure 4.7**. From the plot it can be identified that mechanical alloying for 4 hours has successfully produced Ti-Mg alloys, because Mg peaks are not presence onto the traces indicating that Magnesium powder has well mixed into Titanium powder.

Results also showing that mechanical alloying has caused Ti XRD peaks broadening, as shown in **Figure 4.7** where after milling Ti-0Mg the peaks become less intense and wider compare to that initial Ti powder. Addition of Mg also leads to XRD peaks broadening, as can be seen from the plots, the peak broadening increases as magnesium content increase from 2.5-10wt%, and indicating that there is an interaction between Mg and Ti powders, causing the peak broadening. This broadening is due to mechanical alloying, which has refined the particles size, and addition of Mg to Ti has leads to a grain refinement and a decrease of particle size.

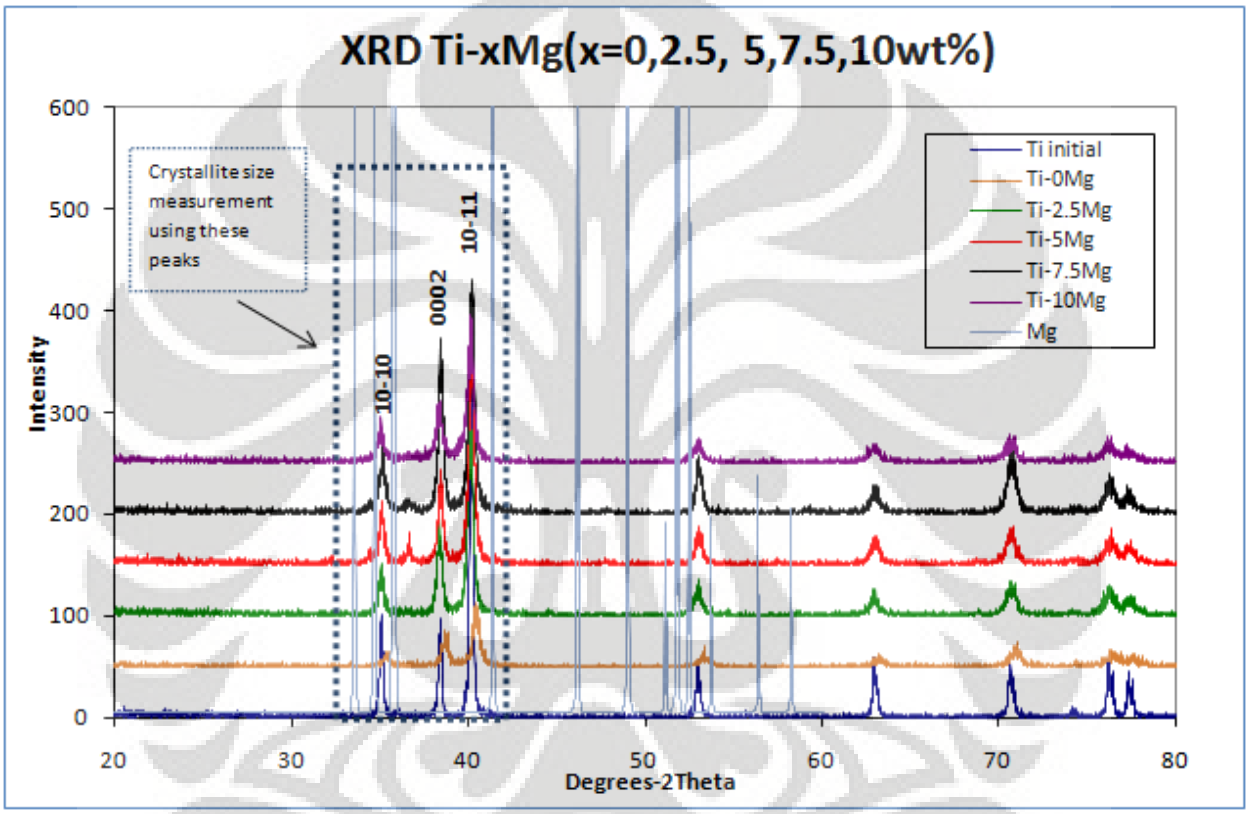

Figure 4.7: XRD spectra of Ti-Mg powder alloys and the peaks chosen for average crystallite size measurement using the Scherrer's formula.

Using this broadening effect, it was also attempted to measure the final crystallite size using Scherrer's formula. To measure average crystallite size using Scherrer's formula, three major peaks in Ti XRD system were used as marked on **Figure 4.7**. The calculated crystallite diameters are given in **Table 1**. Then by plotting average crystallite size with content level of Magnesium (**Figure 4.8**), it is seen that as level of Mg increased the grain size decreases. Result also shows that Ti-7.5Mg has the smallest grain size among others. However, this prediction may not be accurate because the effects of lattice strain have not yet taken into account.

To measure the average crystallite size accurately, the effect of lattice strain must be subtracted, and other effects such as broadening due to machine sources, beam divergence, and sample size must also be subtracted. The lattice strain effect could be analyzed or subtracted by using Williamson-Hall analysis approach (**Equation 4.1**).

$$\beta \cos \theta = \lambda / D_v + 4\varepsilon_{strain} (\sin \theta) \quad \ldots\ldots\ldots\ldots\ldots\ldots \quad (4.1)$$

And lattice strain effect is analysed by following procedures as follow:

- Plot $\beta \cos \theta$ on y-axis (in radians 2θ)
- Plot $4 \sin \theta$ on the x-axis

Then if a linear fit is obtained from the data, thus some parameters can be extracted

- The crystallite size from the y-intercept of the fit
- The strain from the slope of the fit.

However, although it seems simple to subtract lattice strain effect, but when these procedures were applied to XRD broadening results, the lattice strains on each sample exhibit large differences. In certain alloy, there is no any strain effect, but other has large effect. Actually, mill metal powder will usually exhibit non-uniform strain, and cannot be analysed accurately by XRD broadening. The peak broadening is best applied to anneal and brittle metal where strain is not a concern, and for crystallite measurement it is better to use TEM instead of XRD broadening method. As given in **Figure 4.8**, the plot showing inconsistent results because crystallite size were decreased from 2.5 to 7.5wt%Mg, but then increases again at 10wt%Mg, and clearly shows using XRD for this particular purposes may not provide accurate results.

Table 4.1: Results of crystallite size measurement using XRD broadening technique.

Composition (wt %)	Average Grain Size (nm)
Ti-0Mg	25.68
Ti-2.5Mg	26.26
Ti-5Mg	24.53
Ti-7.5Mg	21.17
Ti-10Mg	23.63

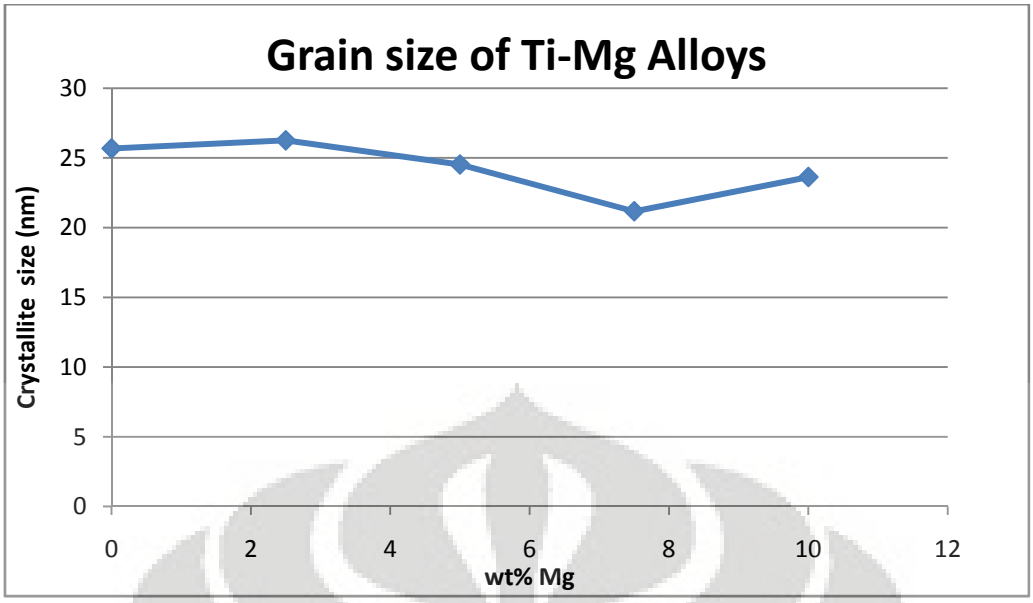

Figure 4.8: Average crystallite size of Ti-Mg alloys; Ti-7.5Mg alloys has the smallest crystallite size.

4.2 ECAP SAMPLES

4.2.1 Density Measurement

Density measurement results from before and after annealing samples are tabulated in table 1. Theoretical density is calculated based on the assumption that all Mg has already dissolved into Ti, and was calculated using **Equation 4.2**. The procedures to obtain theoretical density are discussed in details.

Ti has HCP structure indicating that it has 2 atoms per unit cell, and thus the ideal density given by:

$$\rho = \frac{2atoms}{6.0225x10^{23}} \times at\ wt\ \left(\frac{1}{Volume}\right) \quad \text{.....} \quad (4.2)$$

Where Volume (V) of HCP Ti is given by:

$$V = \frac{\sqrt{3}}{2} \times (a)^2 x\ c \quad \text{.....} \quad (4.3)$$

Where a, c is lattice parameter of Ti.

According to literature [11], the lattice parameters a,c are:

a = 0.00107 (Mg at%) + 2.95103

c = 0.00294 (Mg at%) + 4.70645

Theoretical density in this case is based on atomic percentage, so in order to determine the theoretical density it is important to convert wt% to at%, and it was achieved by using **Equation 4.4 and 4.5**.

$$C_1' = \frac{C_1 A_2}{C_1 A_2 + C_2 A_1} \times 100 \quad \text{..... (4.4)}$$

$$C_2' = \frac{C_2 A_1}{C_1 A_2 + C_2 A_1} \times 100 \quad \text{..... (4.5)}$$

Where:

- C'_1 and C'_2 is atomic percent of Ti and Mg, respectively.
- C_1 and C_2 is weight percent of Ti and Mg, respectively.
- A_1 and A_2 is atomic weights of Ti and Mg, respectively.

Then after converting weight percent into atomic percent, the next step is to determine atomic weight (at wt) fraction as this parameter required in **Equation 4.2**. Then, it is given by:

at wt = (atomic fraction Ti x atomic weight Ti) + (atomic fraction Mg x atomic weight Mg)

It should be noted that the total weight of Ti-Mg powder alloys processed during MA is 10gr. Therefore, by following these procedures, the ideal density after ECAP can be determined, in which assumed that full solubility of Mg in Ti has been achieved.

Table 4.2: Density measurement before and after annealing results.

Alloys (wt %)	Density Before Annealing (g/cm^3)	Density After Annealing (g/cm^3)	Theoretical Density (g/cm^3)	Relative Density Before Annealing	Relative Density After Annealing
Ti-0Mg	4.47	4.52	4.54	0.984	0.995
Ti-2.5Mg	4.33	4.392	4.38	0.988	1.002
Ti-5Mg	4.178	4.23	4.21	0.992	1.004
Ti-7.5Mg	4.07	4.22	4.09	0.995	1.031
Ti-10Mg	3.89	4.21	3.907	0.997	1.077

The density results are being plotted as given in **Figure 4.9**, and this plot showing that before annealed the samples, the density of Ti decreases as level of magnesium increases from 0 to 10wt%, and this results is exactly as expected. Then after annealed the samples, the density slightly increase, but at high level of Mg it seems that the density of 7.5 and 10wt% Mg almost identical to that 5wt%Mg.

Also given is the plot of relative density versus level of magnesium on annealed and un-annealed samples (**Figure 4.10**). Relative density before annealing shows that ECAP has been very effective in consolidating the powders, and ECAP has produced quite fully dense samples and nearly achieve density as predicted theoretically. It also appears that after annealing the samples, the relative density increases slightly and it has produced fully dense samples. These will be discussed further later on.

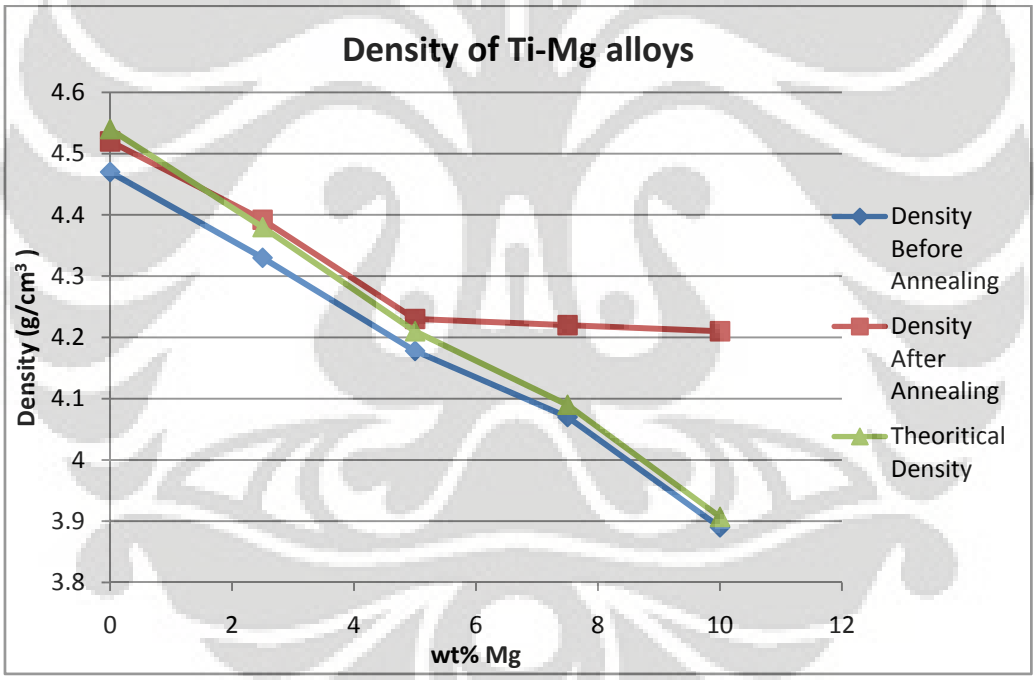

Figure 4.9: Density of Ti-Mg alloys along with its predicted theoretical density.

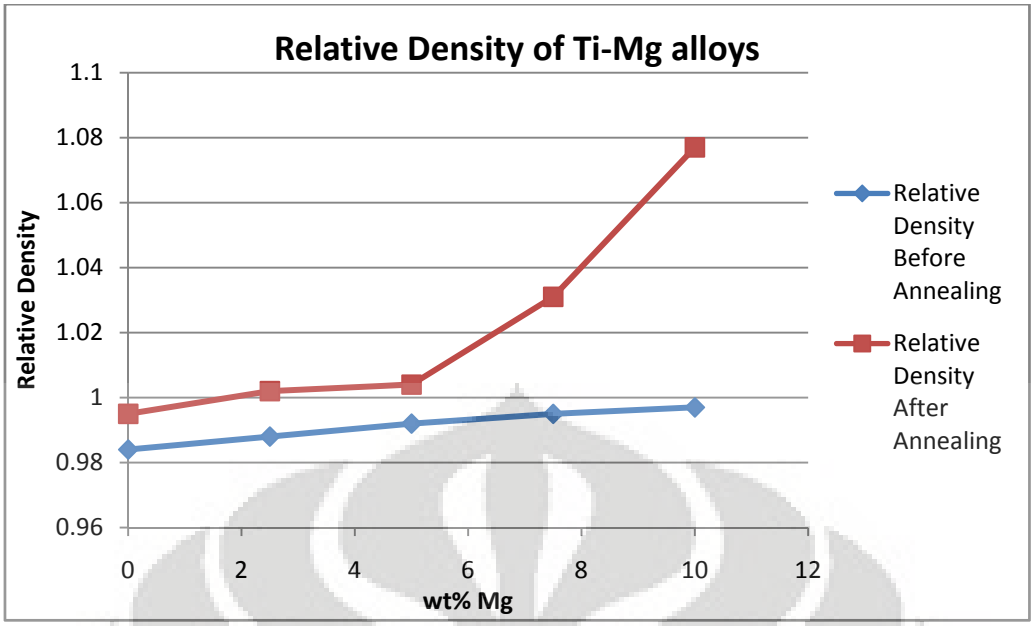

Figure 4.10: Relative density of Ti-Mg alloys.

Result has found agreement with literature, because the density of Ti does reduce after alloying addition with Mg. The density reduce due to additions of Mg have created lattice distortion, and expand the lattice of Ti and combined with Mg having lower atomic weight.

The density slightly increased after annealed the samples, indicating diffusion has occurred. Meanwhile, some strange results appear on Ti-7.5Mg and Ti-10Mg, because the density is almost similar to that Ti-5Mg. This could be due to, in these particular compositions, the Mg content actually has decreased after annealing, so it can be said the composition is no longer 7.5 and 10, but has reduced to somewhere around 5wt%Mg. However, it is possible that some Mg were evaporated during annealing of these two samples because the inside of the quartz tube was coated with a thin dark layer, and cause the density almost identical to 5wt%Mg.

Relative density is representing the number of porosity present, after ECAP results has showing that relative density of each samples in not less than 98%, suggesting that ECAP has effectively produced quite fully dense samples. After annealing, fully dense samples have been obtained, and even more dense than expected. Oxygen may interfere during annealing, and causes the formation of oxide, but the risk of this happening was minimised by heat treating in argon atmosphere. Another possibility is for a Ti-Mg + Mg, 2 phase composite, and then theoretical density should be calculated by volume rule of mixtures.

$$\rho = \rho_1 V_{f(1)} + \rho_2 V_{f(2)} \quad \text{..... (4.6)}$$

However, this leads to a difference in density of less than 1%. Vaporisation therefore is the most likely caused of the relative density increase after annealing.

4.2.2 Microstructure Observation

Figure 4.11 to 4.16 are representing the images of Ti-Mg alloys bulk samples, and these images were taken using SEM for both un-annealed and annealed condition.

A. Un-annealed samples

Figure 4.11 (a) is showing the structure of Ti-0Mg, and there is no significant pattern that can be observed here, particles boundaries cannot be seen, but most important that there is no porosity appears here.

Meanwhile, inter-particles boundaries produced after ECAP are clearly visible in Ti-xMg (x= 2.5, 5, 7.5, 10). The particles boundary example is marked (X) in **Figure 4.12**. These images explained that mechanical bonds between particles produced after ECAP at 400^0C. Some black areas that may represent magnesium still appear on the microstruture, they tend to stay on the boundaries areas as marked (Y) in **Figure 4.12**. As level of Mg increase, there are more Mg stay on the particles boundaries areas. Some of these dark areas however are also residual porosity (between 1-1.5% at low Mg level). At 10%Mg density measurement indicate very little porosity but picture shows a higher level of porosity and defects.

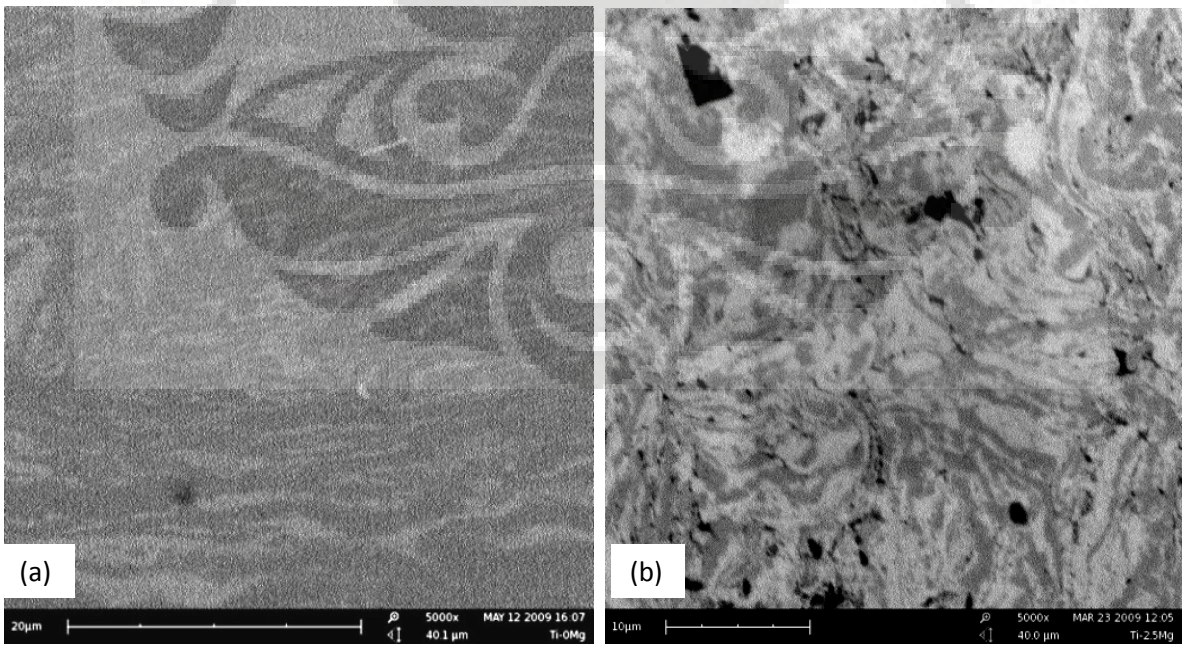

Figure 4.11: SEM microstructure of (a) Ti-0Mg and (b) Ti-2.5Mg of after ECAP alloy in heavily deformed area.

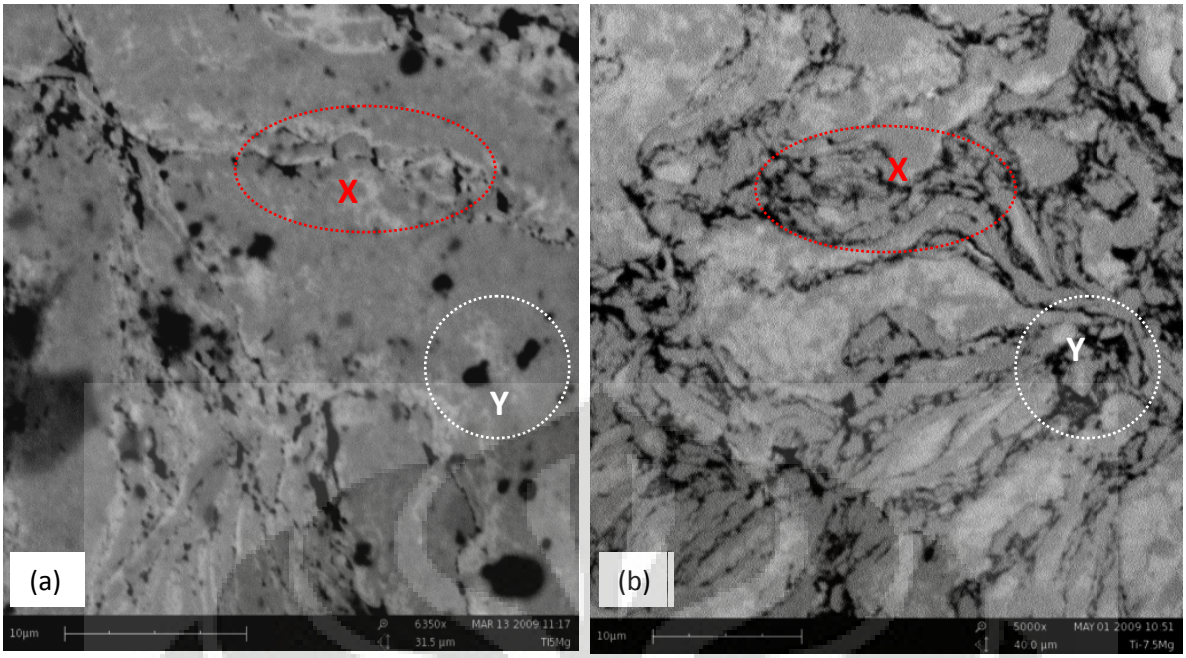

Figure 4.12: After ECAP sample SEM microstructure of (a) Ti-5Mg, and (b) Ti-7.5Mg in heavily deformed area with two regions marked (X) particle boundary, and (Y) magnesium or possibly residual porosity.

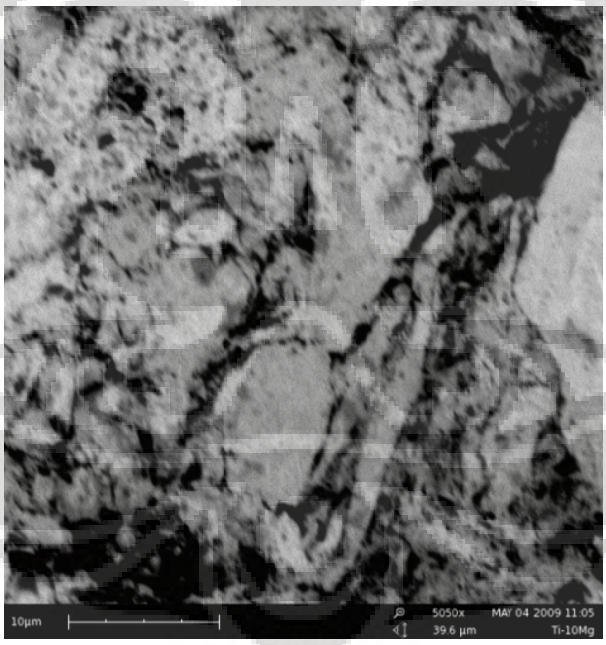

Figure 4.13: SEM microstructure of Ti-10Mg in heavily deformed area.

B. Annealed Samples

The images from after annealed samples showing some improvement in particles boundaries, because the particles boundaries are not clearly visible compare to after ECAP samples. However, in Ti-0Mg (**Figure 4.14 (a)**) the microstructure is just identical

to that after ECAP Ti-0Mg (**Figure 4.11 (a)**). Annealing was done at 600^0C for 1 week, and in the alloys, it has improved the bonding between particles significantly.

Apart from improvements in particles bonding, annealing also causes Mg segregate or separate from Ti, this can be seen from each image of Ti-Mg (2.5-10wt %) after annealed, segregation occur more as the level of Mg increased. This is seen as the irregular dark areas as marked (Z) in **Figure 4.15**. Careful inspection shows that these dark areas are not porosity in this annealed condition. Initially, it was expected to have stable solid solution when performed annealing at 600°C, but instead it causes Mg to segregate, and as the result we may produce two phases composites of Ti-Mg +Mg rather than alloy. The segregation may have effect on the mechanical properties.

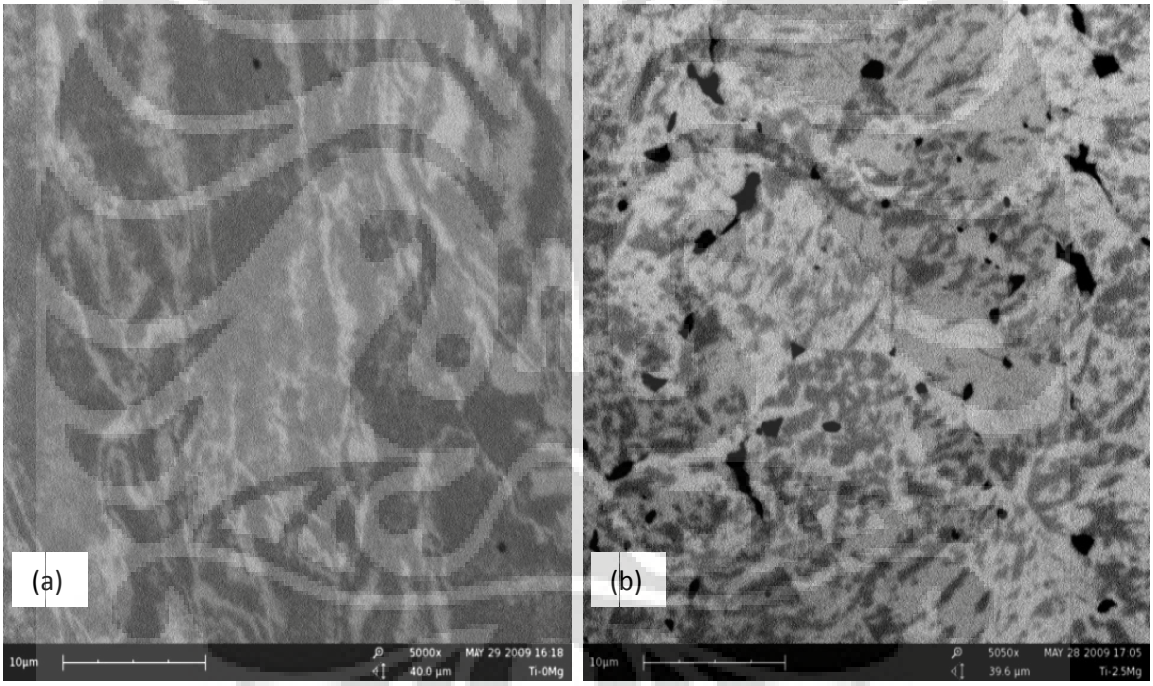

Figure 4.14: SEM microstructure of (a) Ti-0Mg and (b) Ti-2.5Mg ECAP-ed alloy after annealing at 600°C for 7 days in heavily deformed area.

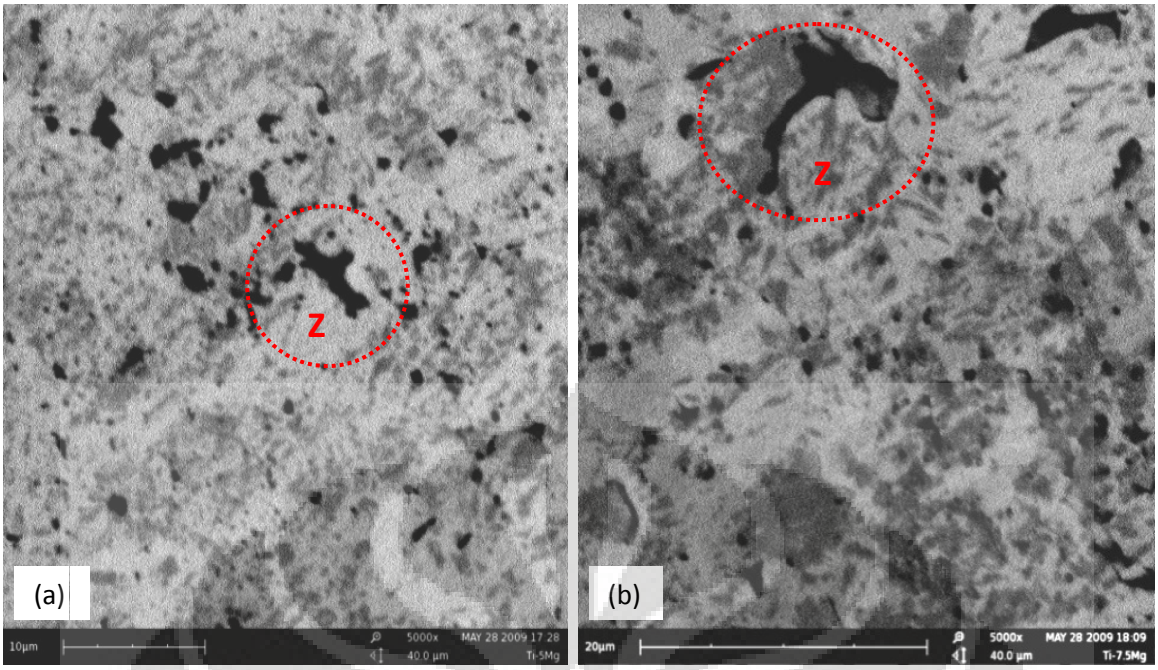

Figure 4.15: SEM microstructure of (a) Ti-0Mg and (b) Ti-2.5Mg ECAP-ed alloy after annealing at 600°C for 7 days in heavily deformed area. Dark area marked (Z) is magnesium which segregate as the result of annealing.

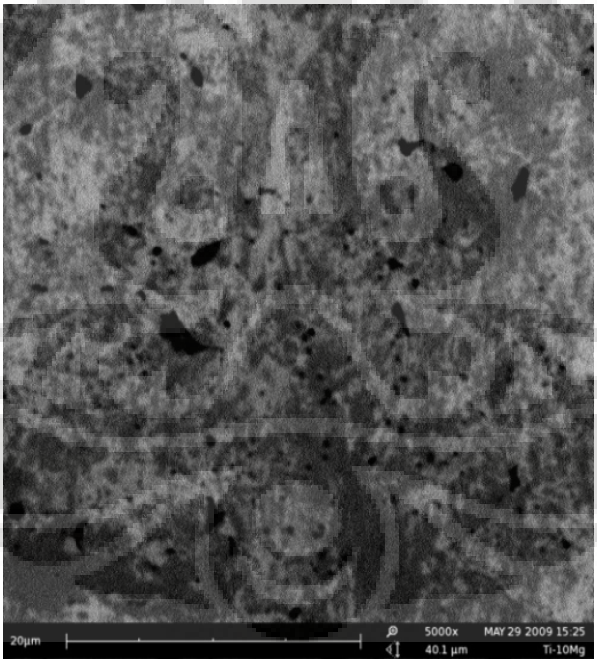

Figure 4.16: SEM microstructure of Ti-10Mg ECAP-ed alloy after annealing at 600°C for 7 days in heavily deformed area.

4.2.3 Ball Indentation Test (BIT)

A plot of load versus extension of the raw data obtained from the ball indentation test would look like as displayed in **Figure 4.17**. There are 8 load and unload cycles involved in each test with the initial load 100N and an increase of 100N in each cycle. The full raw data plots achieved from BIT are provided in **Appendix II**.

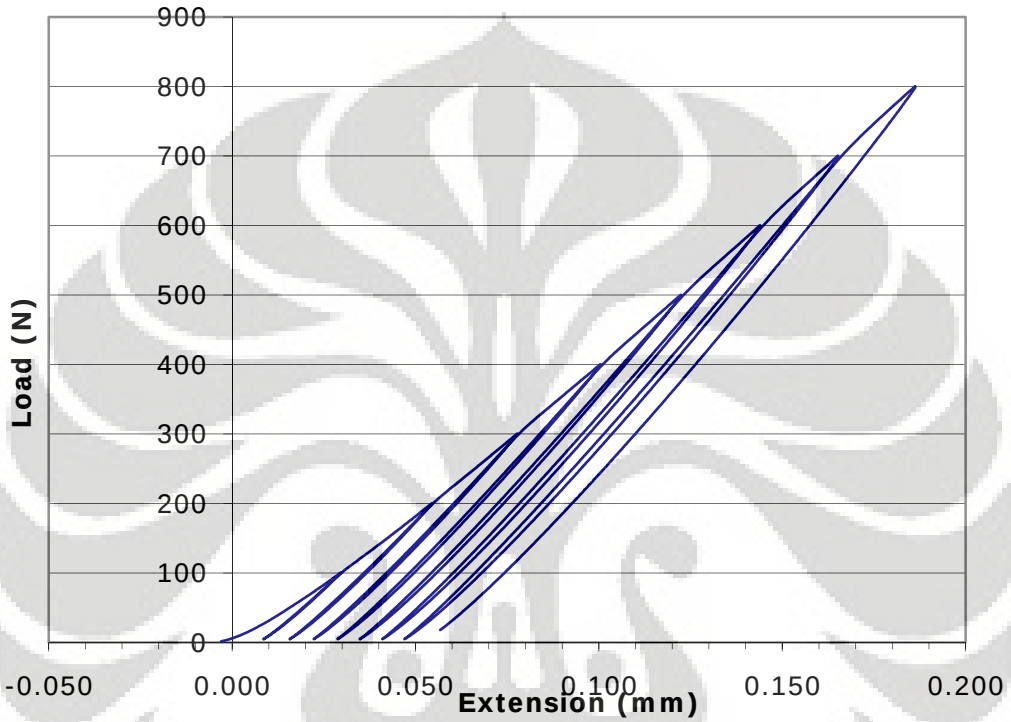

Figure 4.17: Plot of raw data from BIT.

Each load/unload cycle must be analysed one by one, and four important parameters are required to be collected from the data, which are:

1. W : The load at the peak of cycle (N)
2. h_t : the total extension of cycle (mm)
3. h_p : the plastic extension
4. S : the gradient of tangent line constructed from the initial unloading response, and it is used to determine reduce modulus E.

These parameters must be determined by analysing each cycle, however, S parameter is only collected from the first cycle, and should not be calculated once work hardening has begun. It is a measure of elastic response of the alloy.

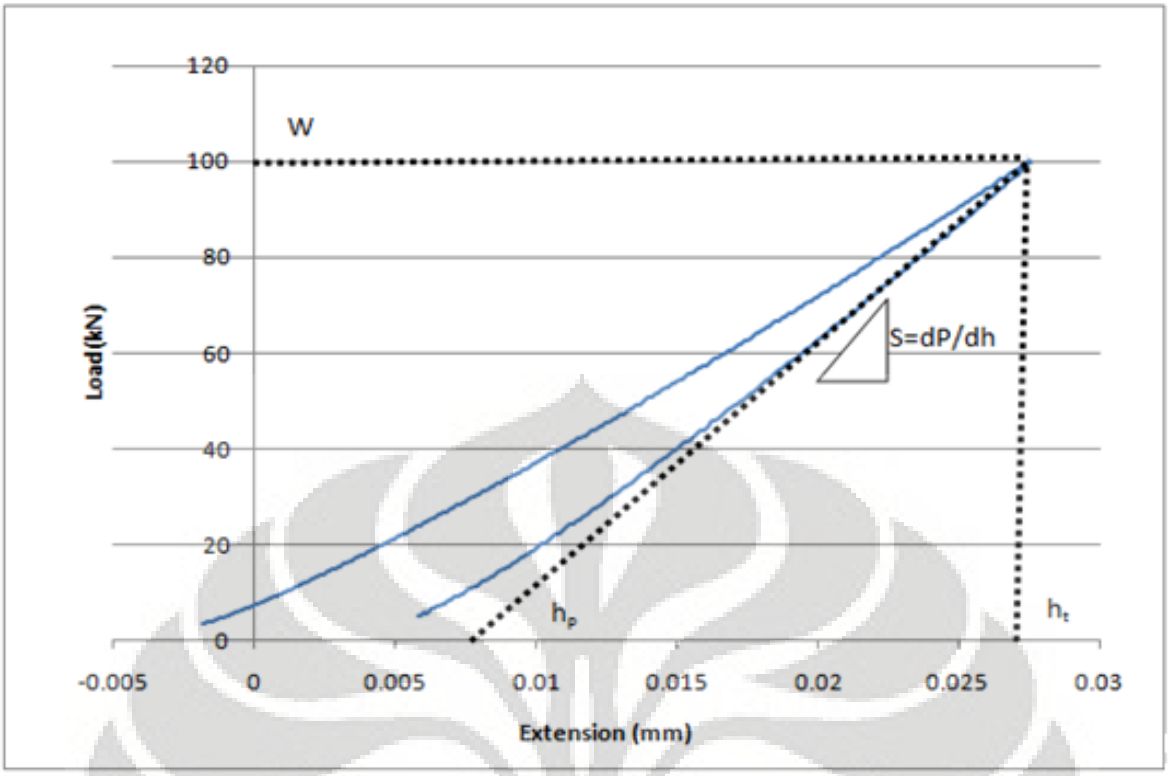

Figure 4.18: A single cycle and important parameters to be determined.

Then after collecting W, h_t, and h_p, calculate stress and strain using equation:

Stress, $P_m = W/\pi a^2$ ..... (4.7)

Strain, $\varepsilon = 0.2a/R$ ..... (4.8)

Where R is the radius of the indenter, while a is the contact radius at peak load.

Ideally, at peak load, the indenter will penetrate into material and remain in contact with the indenter all the way to the surface as shows in **Figure 4.19(a)**, but in reality that is not always the case, instead some displacement at the surface occurs and the surface in contact with the material is slightly less than expected. Thus contact radius can be defines as the actual area of the material in contact with the indenter (**Figure 4.19 (b)**), and calculated from the contact depth, h_c.

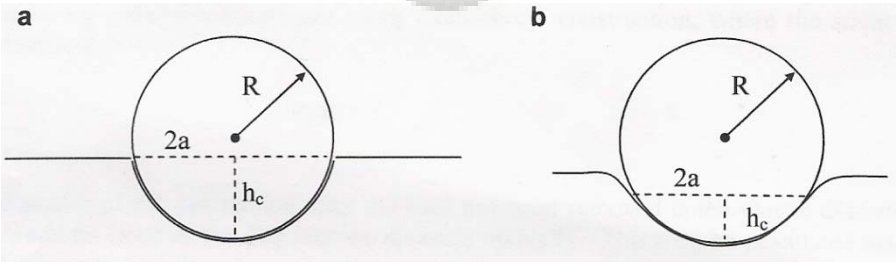

Figure 4.19: a) Perfect or ideal indentation situation; b) the real case of indentation situation

The contact depth is a function of the indenter geometry, and due to the indenter having spherical shape, therefore, it is given by **Equation 4.9**.

$$h_c = h_t - 0.75\,(h_t - h_p) \quad \text{..... (4.9)}$$

The contact diameter is determined using **Equation 4.10**; with work hardening (n) function is taken into account:

$$a^2 = \frac{5(2-n)(2Rh_c - h_c^2)}{2 + (4+n)} \quad \text{..... (4.10)}$$

To determine work hardening function, an iterative approach is needed. The plot of stress vs strain should be done, and assuming that the material behaviour follows the conventional power law behaviour with an initial guess at n value, and fit power law equation to the curve, as shown in **Figure 4.20** below. The 'fitted' n value is then used to plot the next iteration.

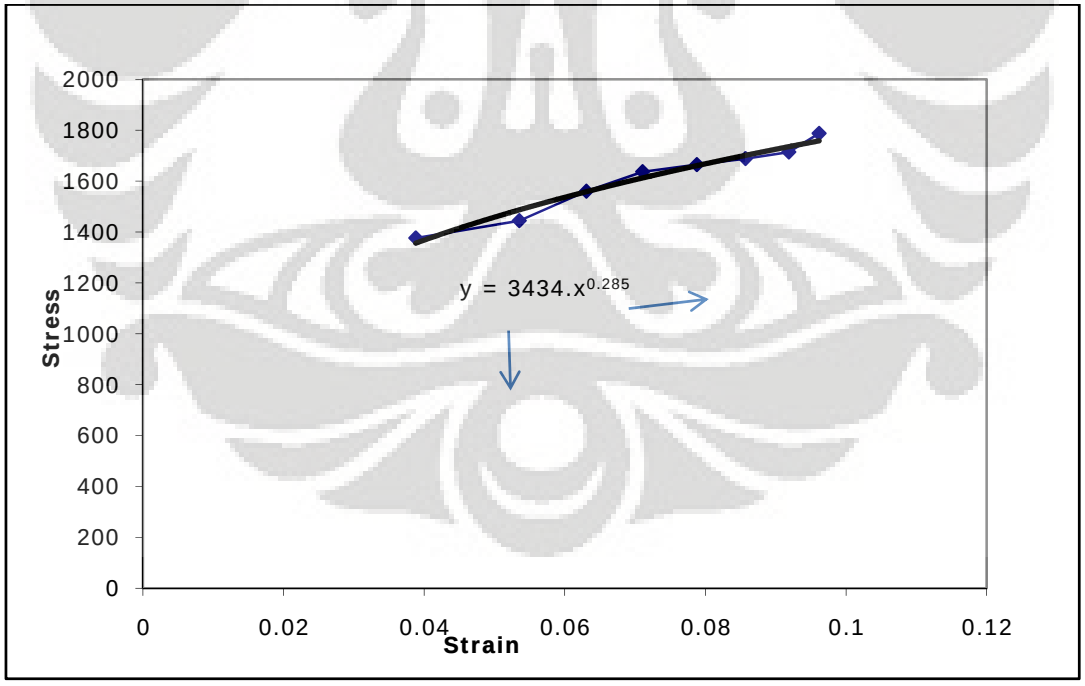

Figure 4.20: Determination of work hardening parameters

Then, the analysed results are given in **Figure 4.21 and Figure 4.22**, which represent un-annealed and annealed samples respectively. These result shows some inconsistency, for

instance in **Figure 4.21** shows that the strength of Ti-7.5Mg is higher than Ti-2.5Mg and Ti-5Mg, but at the same time the strength of Ti-10Mg is lower than Ti-7.5Mg.

Mechanical properties measurement result suggesting that after ECAP or before annealing the strength of Ti-Mg bulk alloys is most likely dominated by the inter-particles bonding achieved in ECAP. The strength of these particular samples is independent of alloying; meaning that Mg alloying addition in Ti does not contribute to the strength of these particular samples.

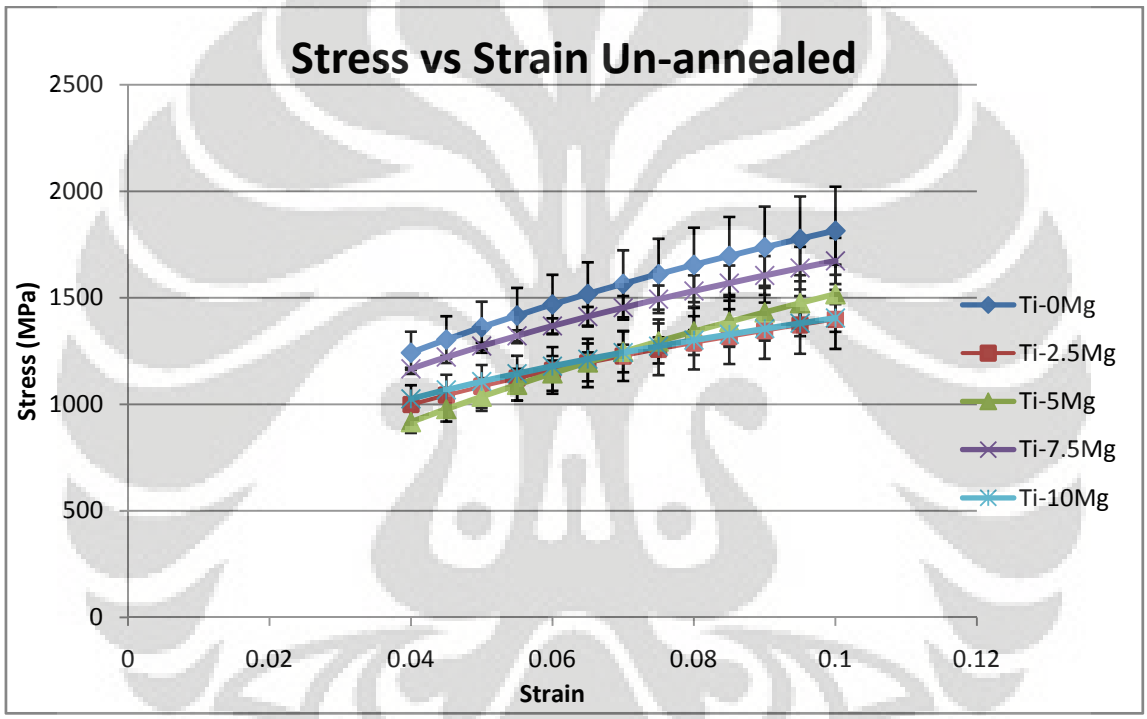

Figure 4.21: Un-annealed samples strength

After annealing the strength of some compositions (2.5 and 7.5wt%Mg) greatly improved which indicated strengthening, on the other hand, for the others compositions annealed seems not improved the strength significantly, suggesting the results are inconsistent, thus required further evaluation. Annealing is expected to give softening as well as strengthening effect. The softening effect mainly because annealed would remove any deformation or removing any internal strain that may occurred after ECAP, while strengthening effect is because annealing has improved the inter-particles boundaries as already shown on SEM microstructure image of this particular conditions. Thus there are 2 competing effects which

would dominate the strength, but it cannot be predicted which will dominate more. It is also possible that the segregation of Mg which occur after annealing interferes with the strength of these Ti-Mg alloys, so the probability of performing indentation on the areas rich of Mg content may be a reasonable explanation on why in some compositions the strength have not improved significantly. Therefore, to have better understanding on these results, it would be very helpful to repeat some stage of experiment.

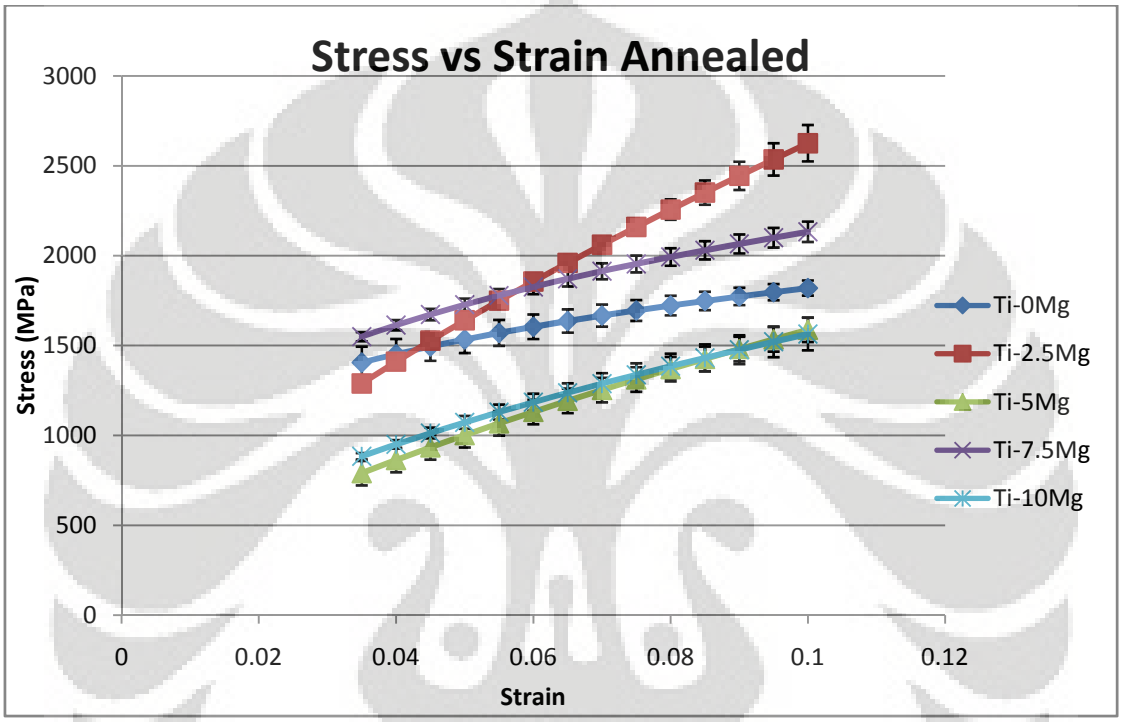

Figure 4.22: Annealed samples strength

In **Figure 4.23**, the strength at a strain of 0.09 is plotted against the nominal Mg content. This chart has proved that the results are inconsistent, and would require further evaluation. In addition, as given in **Figure 4.23** which indicates the BIT results of CP-Ti, shows that the strength of Ti-0Mg (or can be said as Ti-as milled) prepared by MA and ECAP is higher than the strength of CP-Ti sheet. It has been known that MA and ECAP processes normally leads to grain refinement, and although the results still showing some inconsistency, it was obtained results consistent with Hall-Petch relationship which is the strength become higher as the grain size smaller. Therefore, these two processes (MA and ECAP) have greatly improved the strength of Ti.

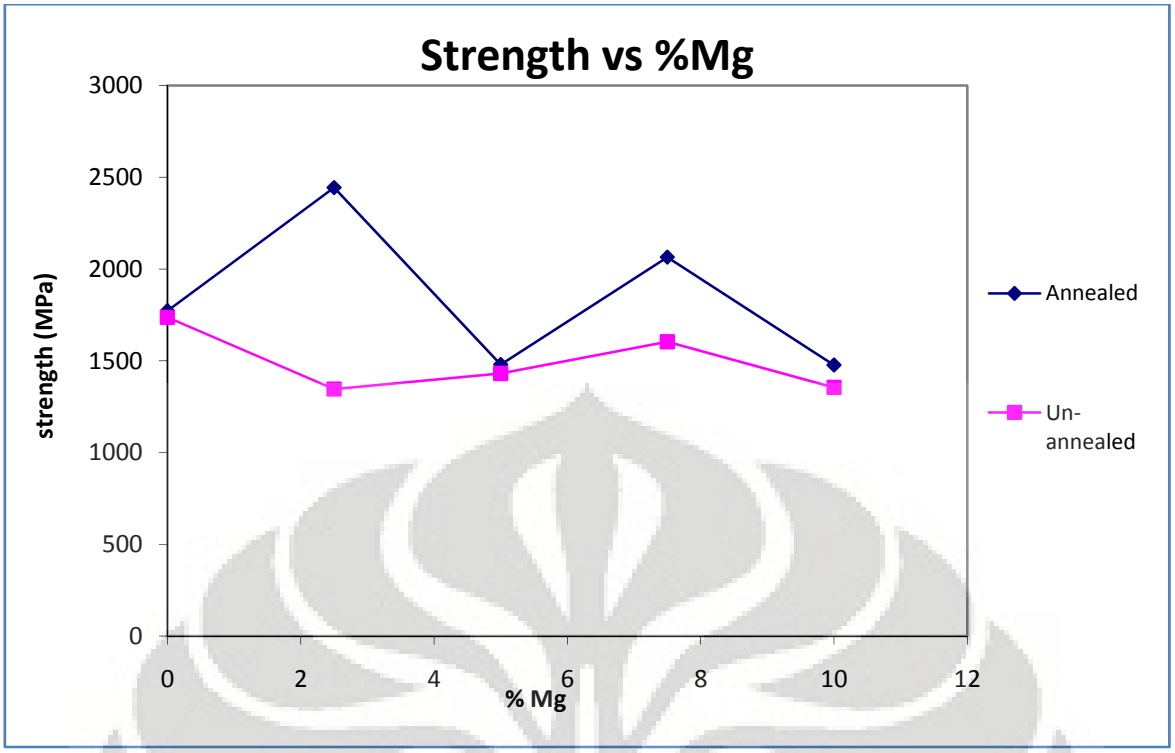

Figure 4.23: Strength comparison of annealed and un-annealed samples vs level of Mg.

CHAPTER V
CONCLUSION AND FUTURE WORKS

Based on the result obtained in this project, the following conclusion can be drawn:

1. Mechanical alloying is capable to produce combination of Ti-Mg alloys, but homogeneous structure cannot be achieved at 4hours milling time, and thus longer milling time should be applied in order to achieve better homogeneity. In addition, ECAP gives severe plastic deformation but this also does not give homogenous microstructure.
2. Mechanical alloying and addition of Mg into Ti causes XRD peaks broadening, mostly because MA leads to particles refinement, while addition of Mg leads to particles as well as grain refinement. The final crystallite prediction based on Scherrer's formula may not provide accurate results because the lattice strain effect cannot be extracted appropriately and mostly due to milled powders materials usually exhibit non-uniform strain so cannot be analysed appropriately by XRD broadening. However, a crystallite size of ~30-50nm is possible.
3. Density of Ti greatly decreased as Mg content increases, and Mg may evaporate during annealing and cause the density of Ti-7.5Mg and Ti-10Mg to apparently increase. Relative density is showing that ECAP has produced not less than 98% dense structure. After annealed it was achieved fully dense structure, but oxide formation is possible as the relative density is higher than 100% on each compositions.
4. Observation by SEM has revealed that ECAP has produced interparticles boundaries which are more likely mechanically bonded and these boundaries have improved after annealing performed. Annealing also leads to Mg segregation due to fast diffusion of Mg, and thus produce 2 phases composite of Ti-Mg + Mg.
5. Interparticles boundaries produce after ECAP dominate the strength while addition of Mg seems has no effect on the strength of Ti. Strength increased after annealing, as the improvements in boundaries have been achieved. Mechanical properties results require further evaluation, and the effect of MA and alloying addition of Mg on mechanical properties is not well understood. Additionally, MA and ECAP significantly improve strength of Ti due to grain refinements.

Based on the study done and result obtained, therefore, some future works that need to be conducted are as following:

1. Mechanical alloying with longer milling time should be performed to achieve more homogenous structure, and increasing the Mg level can be performed too.
2. Determine the grain size of ECAP and annealed materials using TEM.
3. Performing XRD on after annealed samples, just to check how much Mg is remaining.
4. Repeat some stage of project to achieve better understanding on the deformation behaviour. Most important is on ball indentation test, because of the inconsistency in the results obtained.

REFERENCES

[1] Valentin N. Moiseyev, *Titanium Alloys: Russian Aircraft and Airspace Application*, Chapter 1-6, Copyright 2006 by Taylor & Francis Group, LLC.

[2] Joshi V.A, *Titanium Alloys: An Atlas of Structures and Fracture Features*, Chapter 2 (Physical Metallurgy of Titanium Alloys), Copyright 2006 by Taylor & Francis Group, LLC.

[3] J.L Murray, *The Mg-Ti (Magnesium-Titanium) System*, Bulletin of Alloy Phase Diagrams Vol. 7, No. 3, Page 245, 1986.

[4] S. Fusheng, S. Froes, *Synthesis and Characterization of mechanical-alloyed Ti-x Mg alloys*, Journal of Alloys and Compounds 340 (2002) 220-225.

[5] D. M. J. Wilkes, P. S. Goodwin, C. M. Ward-Close, K. Bagnall, J. Steeds, *Solid Solution of Mg in Ti by mechanical alloying*, Materials Letters 27(1995) 47-52.

[6] Suryanarayana. C, Froes. F.H, *Mechanical Alloying of Titanium-Base Alloys*, Advanced Material. 1993, 5, No.2.

[7] Suryanarayana. C, *Mechanical alloying and milling*; Progress in Materials Science 46, (2001).

[8] Furukawa.M, Horita.Z, Langdon.T.G, *Developing Ultrafine Grain Size Using Severe Plastic Deformation,* Advanced Engineering Materials (2001).

[9] R. Lapovok, D. Tomus, B.C. Muddle, *Low-temperature compaction of Ti–6Al–4V powder using equalchannel angular extrusion with back pressure,* Materials Science and Engineering A 490 (2008) 171–180.

[10] M.Moss, R. Lapovok, C. Bettles, *The Equal Channel Angular Pressing of Magnesium and Magnesium Alloys*, JOM, 59(8), page 54-57, (2007).

[11] Ward-Close, Materials Letter VII (8-9).

APPENDIX I

XRD Results

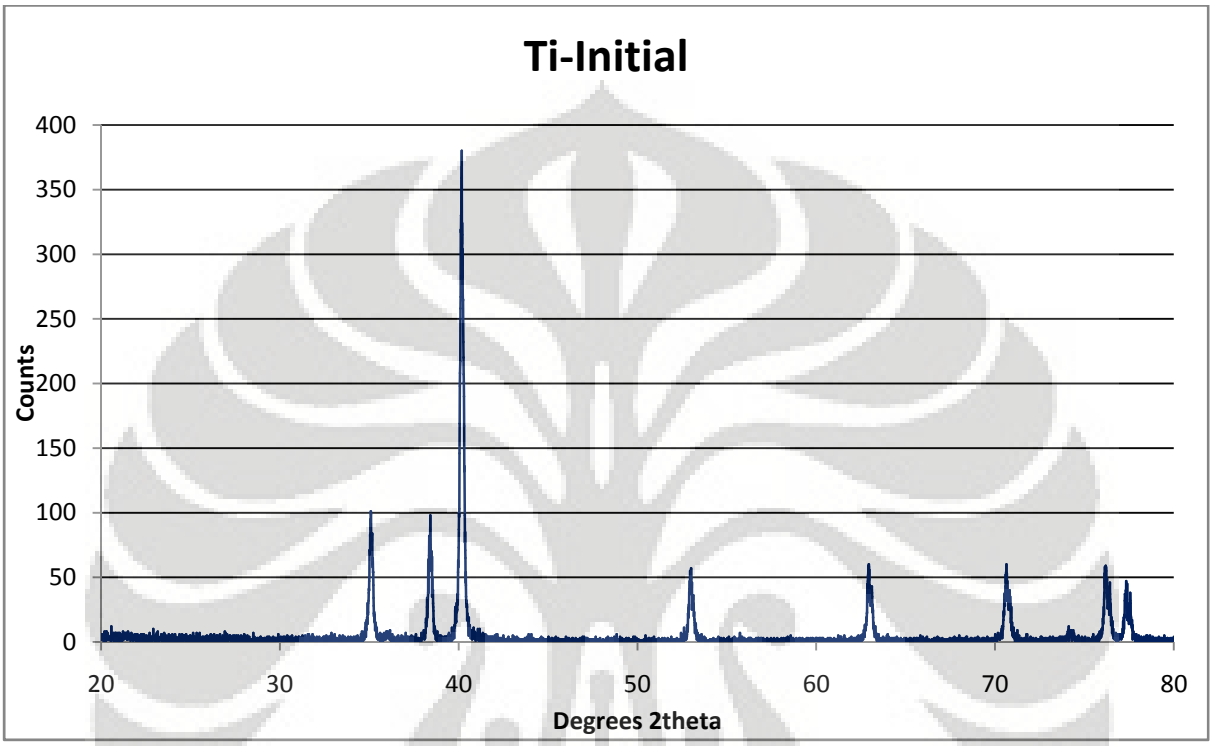

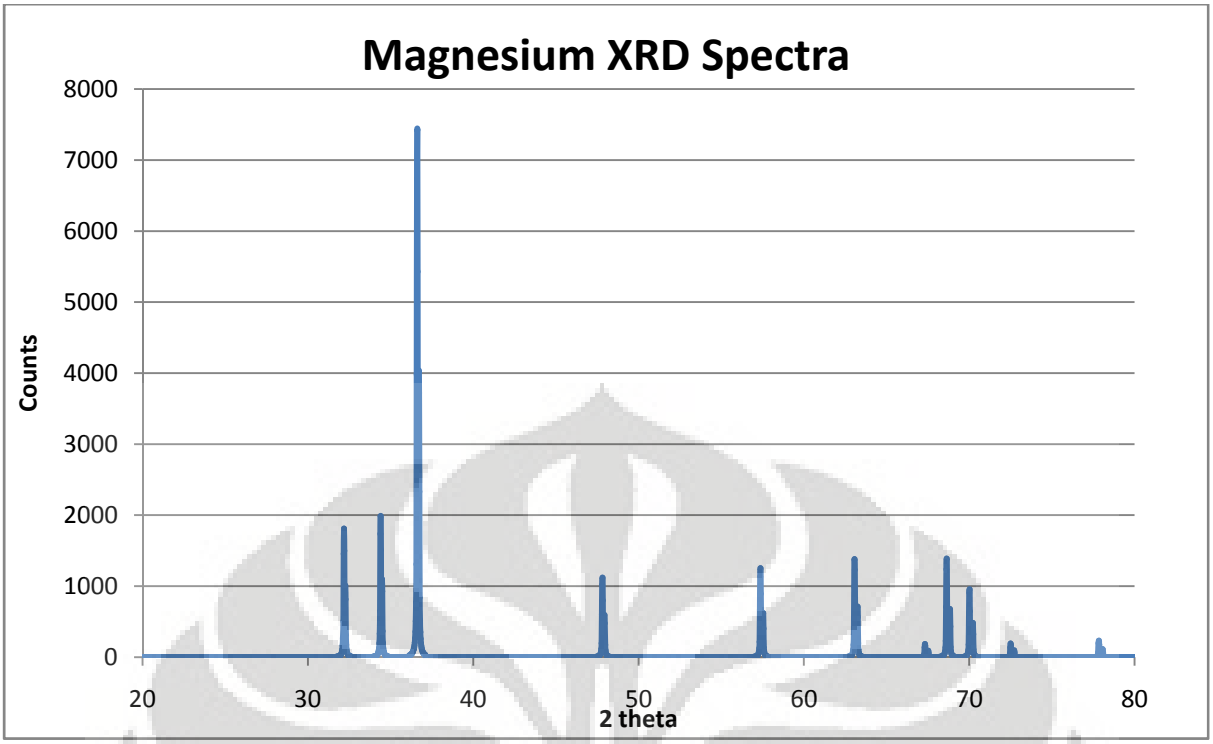
Magnesium XRD Spectra
8000
7000
6000
5000
4000
3000
2000
1000
0
Counts
20
30
40
50
60
70
80
2 theta

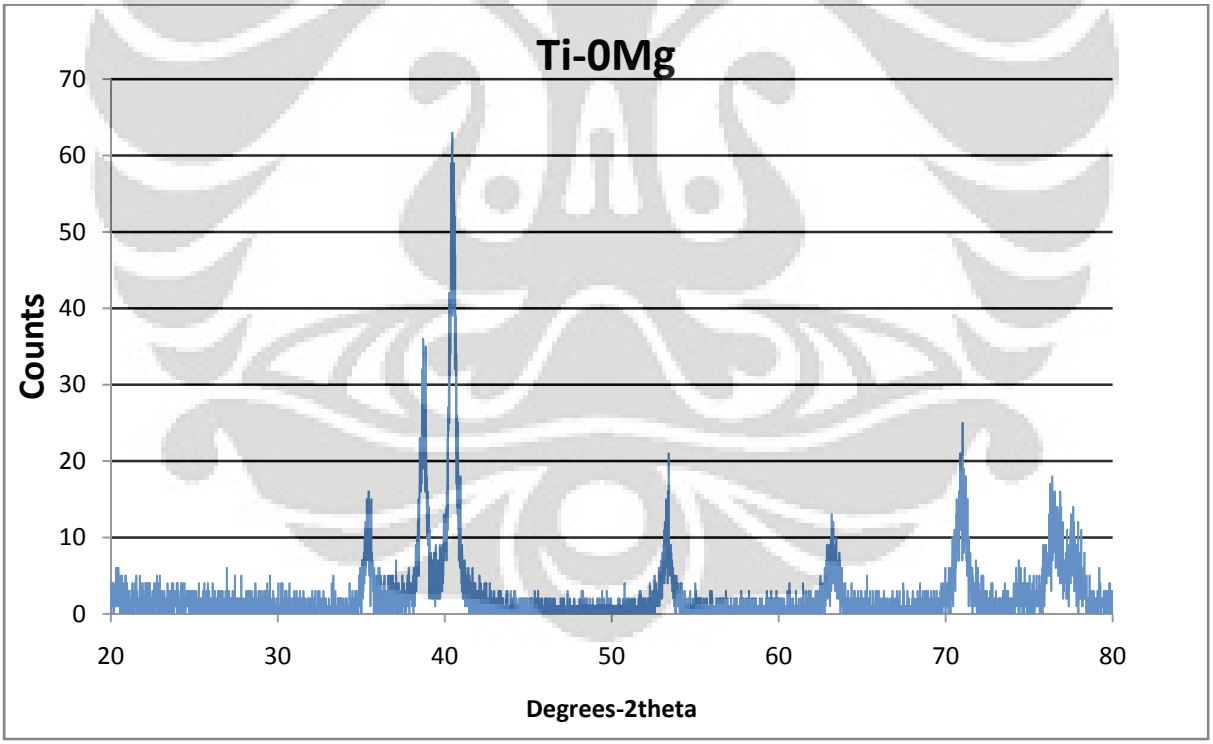
Ti-0Mg
70
60
50
40
30
20
10
0
Counts
20
30
40
50
60
70
80
Degrees-2theta

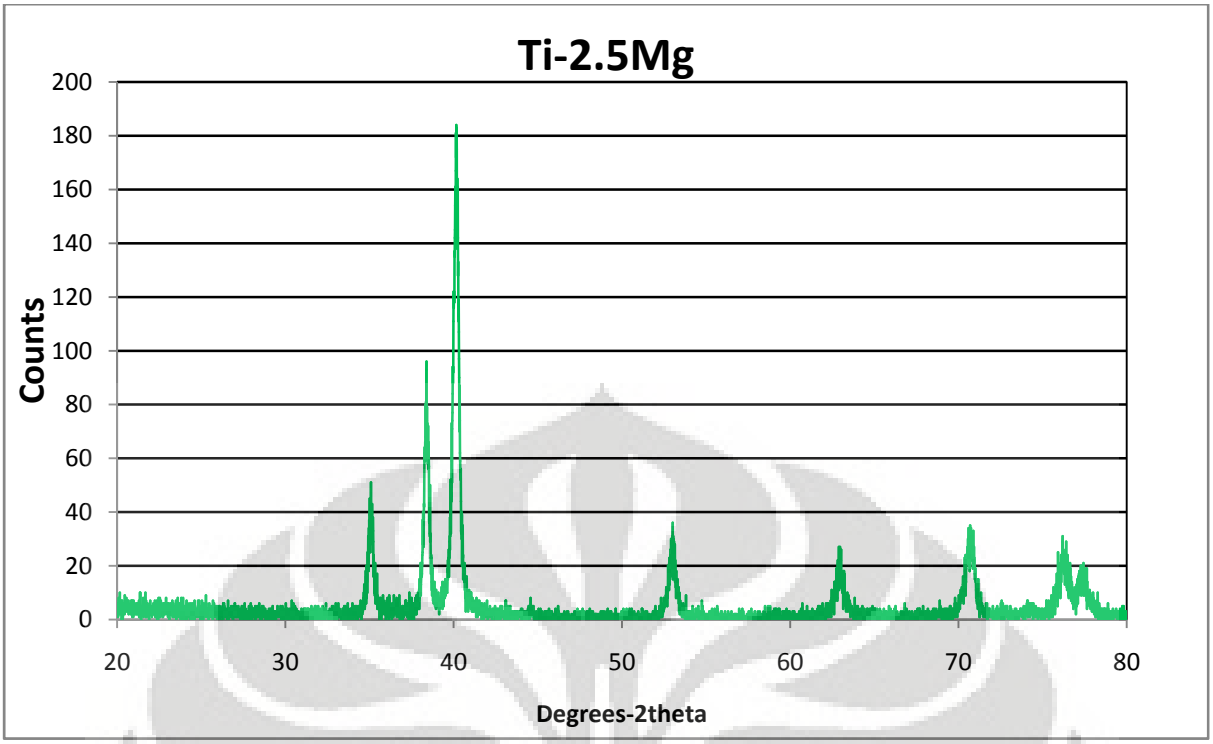
Ti-2.5Mg
Counts
200
180
160
140
120
100
80
60
40
20
0
20
30
40
50
60
70
80
Degrees-2theta

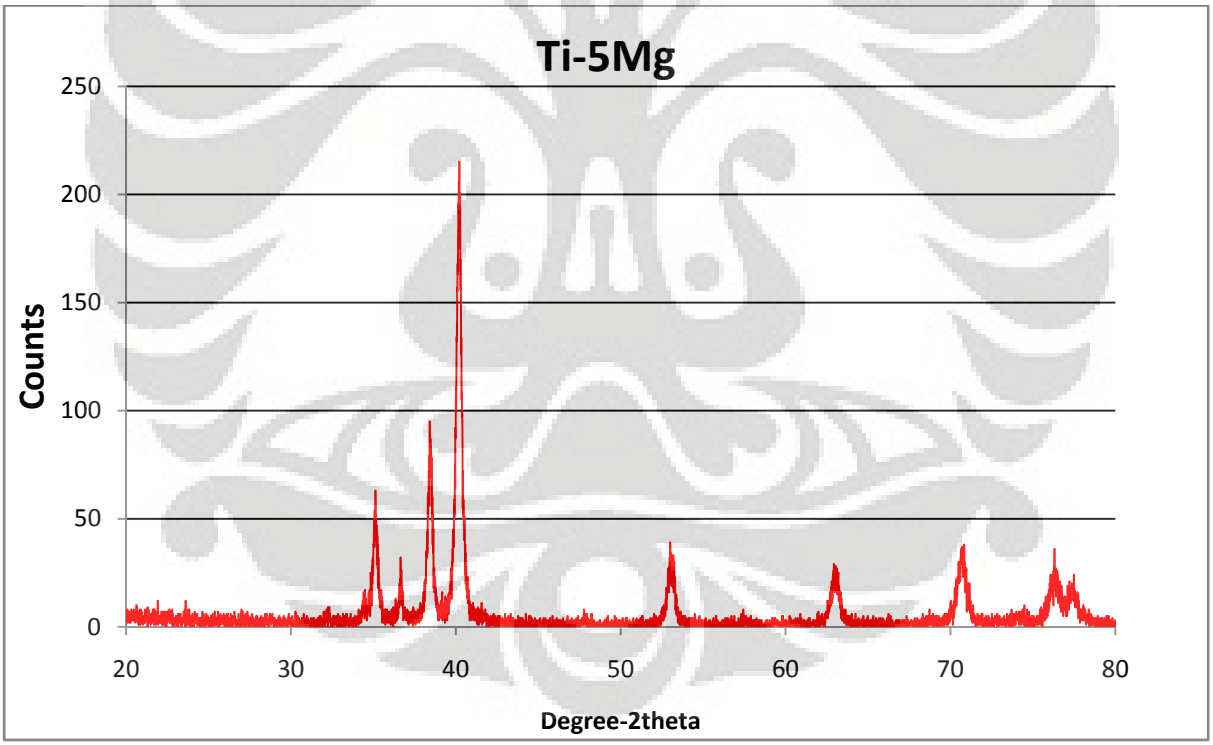
Ti-5Mg
Counts
250
200
150
100
50
0
20
30
40
50
60
70
80
Degree-2theta

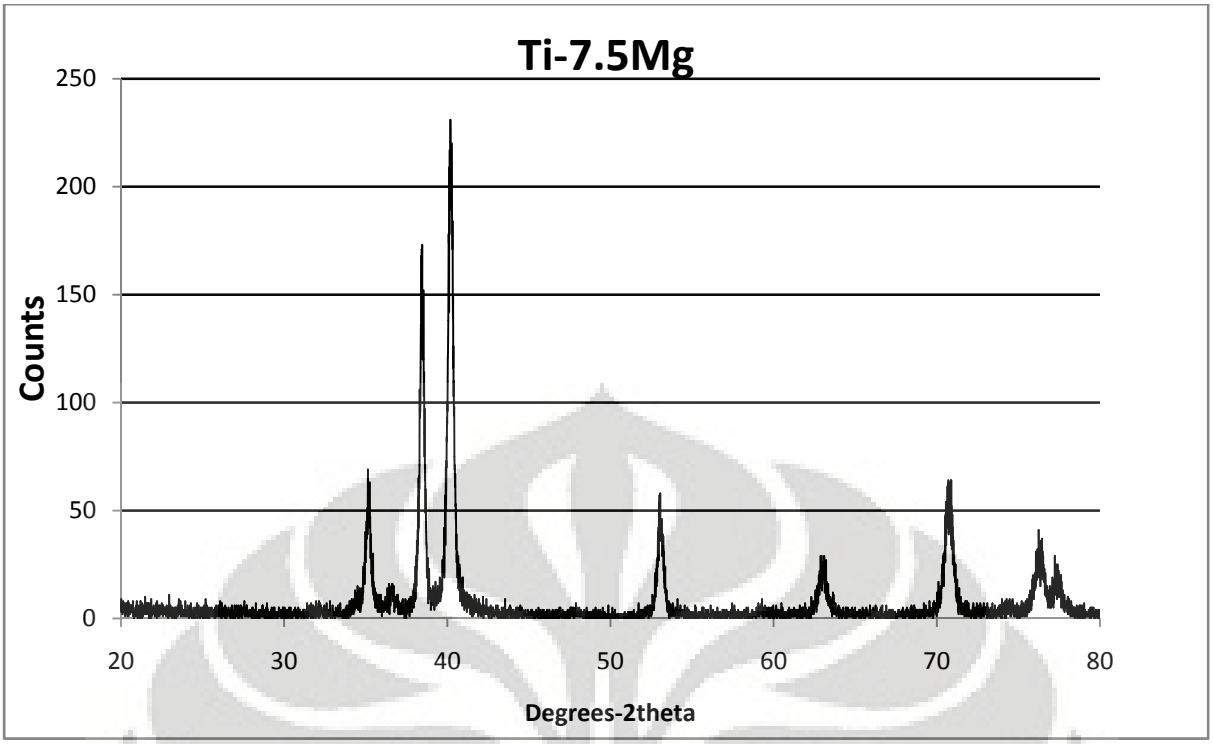
Ti-7.5Mg
Counts
250
200
150
100
50
0
20
30
40
50
60
70
80
Degrees-2theta

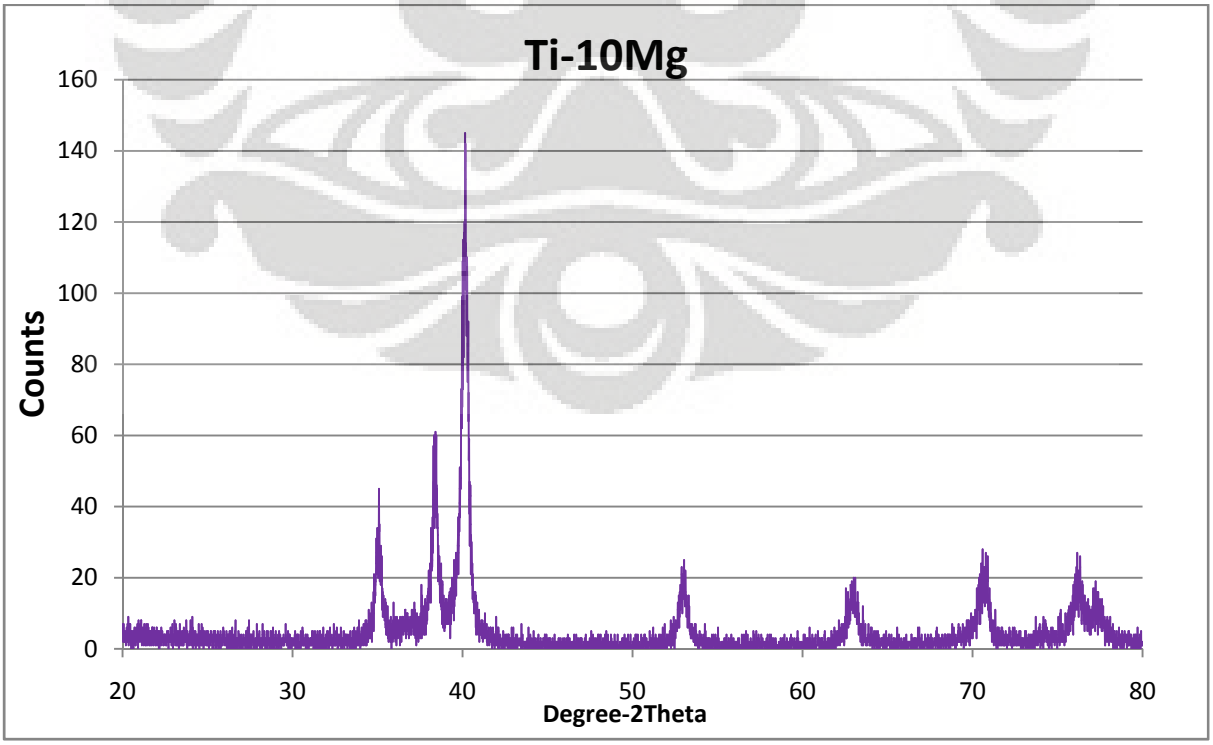
Ti-10Mg
Counts
160
140
120
100
80
60
40
20
0
20
30
40
50
60
70
80
Degree-2Theta

APPENDIX II

Ball Indentation Raw Data

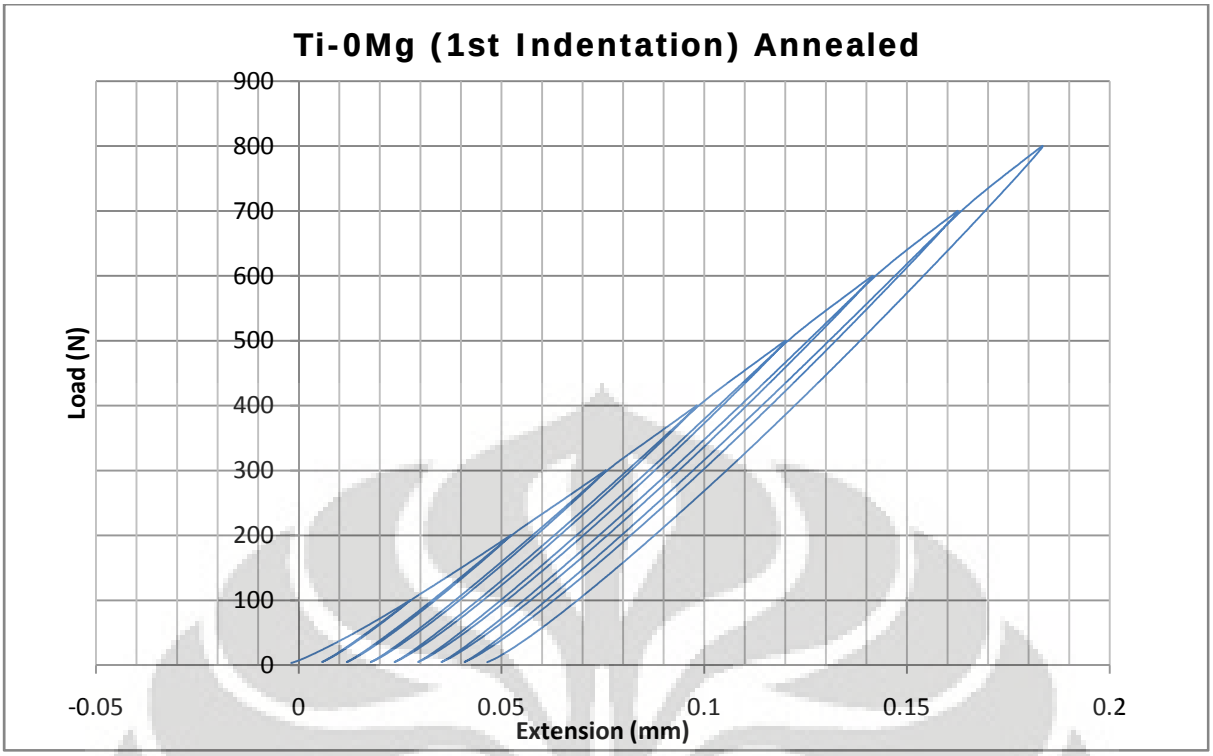
Ti-0Mg (1st Indentation) Annealed
Load (N)
900
800
700
600
500
400
300
200
100
0
-0.05
0
0.05
0.1
0.15
0.2
Extension (mm)

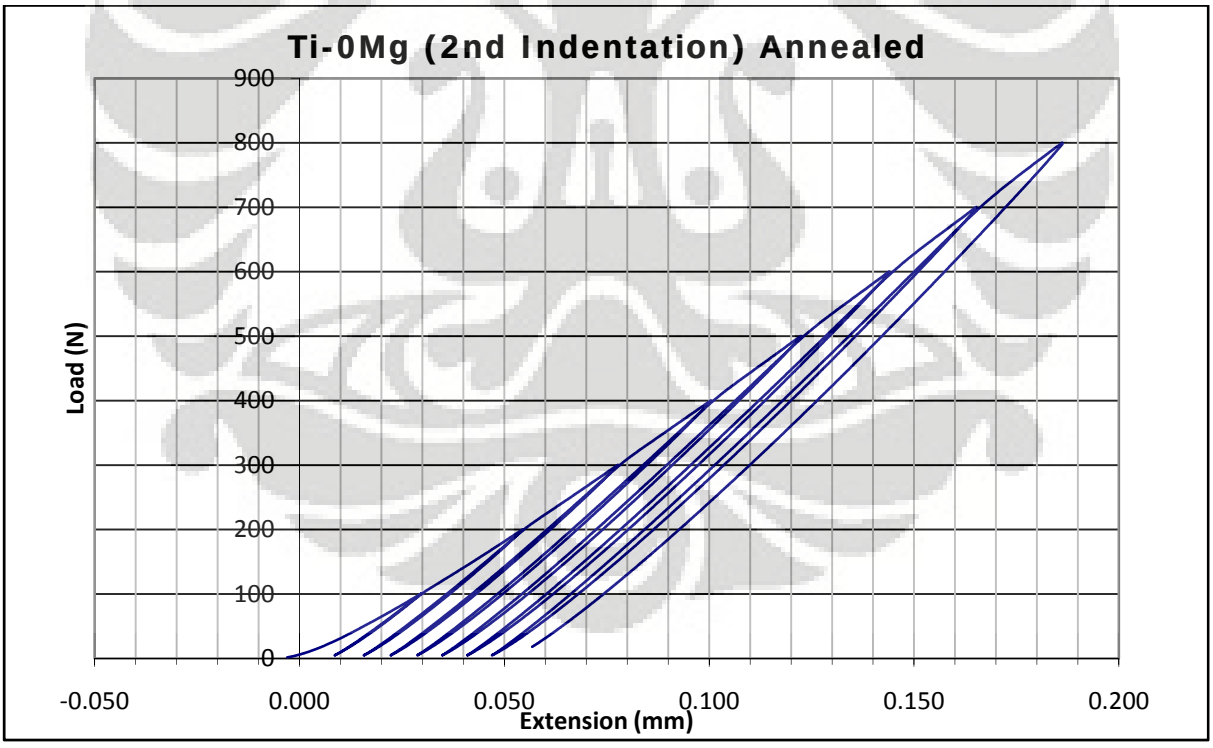
Ti-0Mg (2nd Indentation) Annealed
Load (N)
900
800
700
600
500
400
300
200
100
0
-0.050
0.000
0.050
0.100
0.150
0.200
Extension (mm)

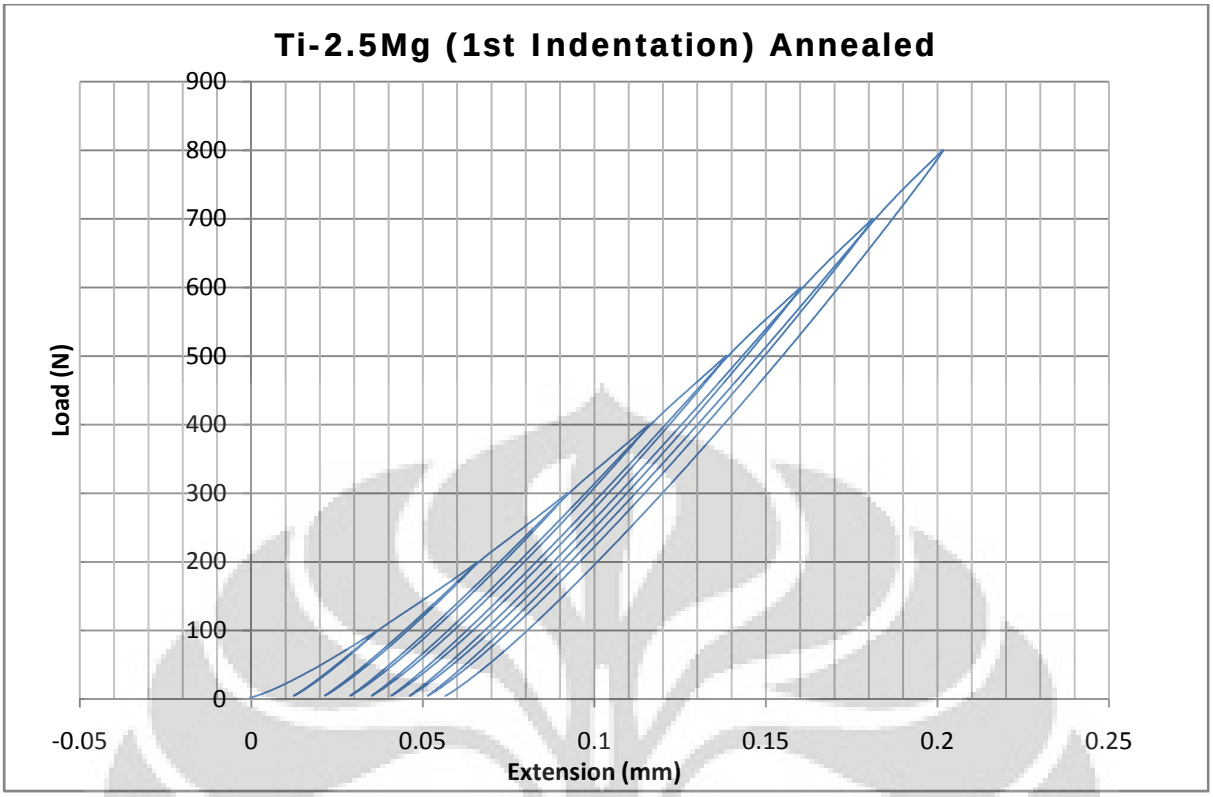
Ti-2.5Mg (1st Indentation) Annealed
Load (N)
900
800
700
600
500
400
300
200
100
0
-0.05
0
0.05
0.1
0.15
0.2
0.25
Extension (mm)

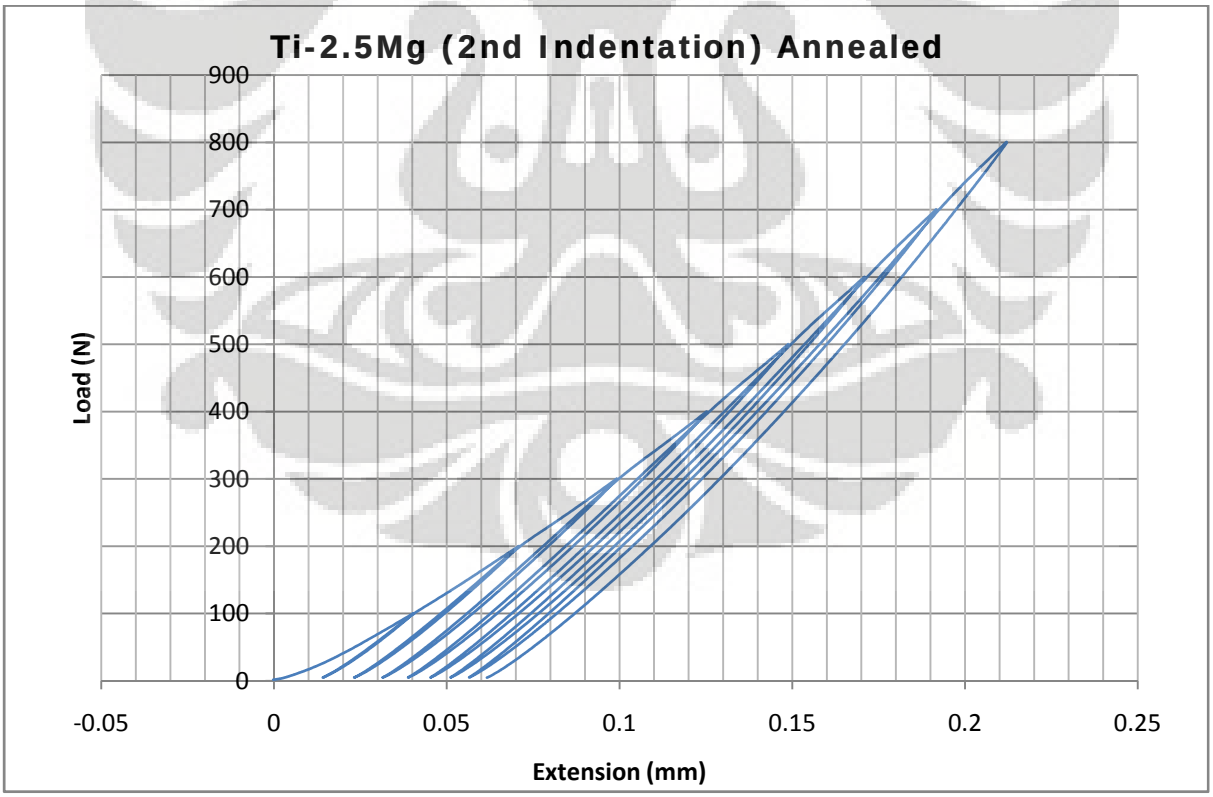
Ti-2.5Mg (2nd Indentation) Annealed
Load (N)
900
800
700
600
500
400
300
200
100
0
-0.05
0
0.05
0.1
0.15
0.2
0.25
Extension (mm)

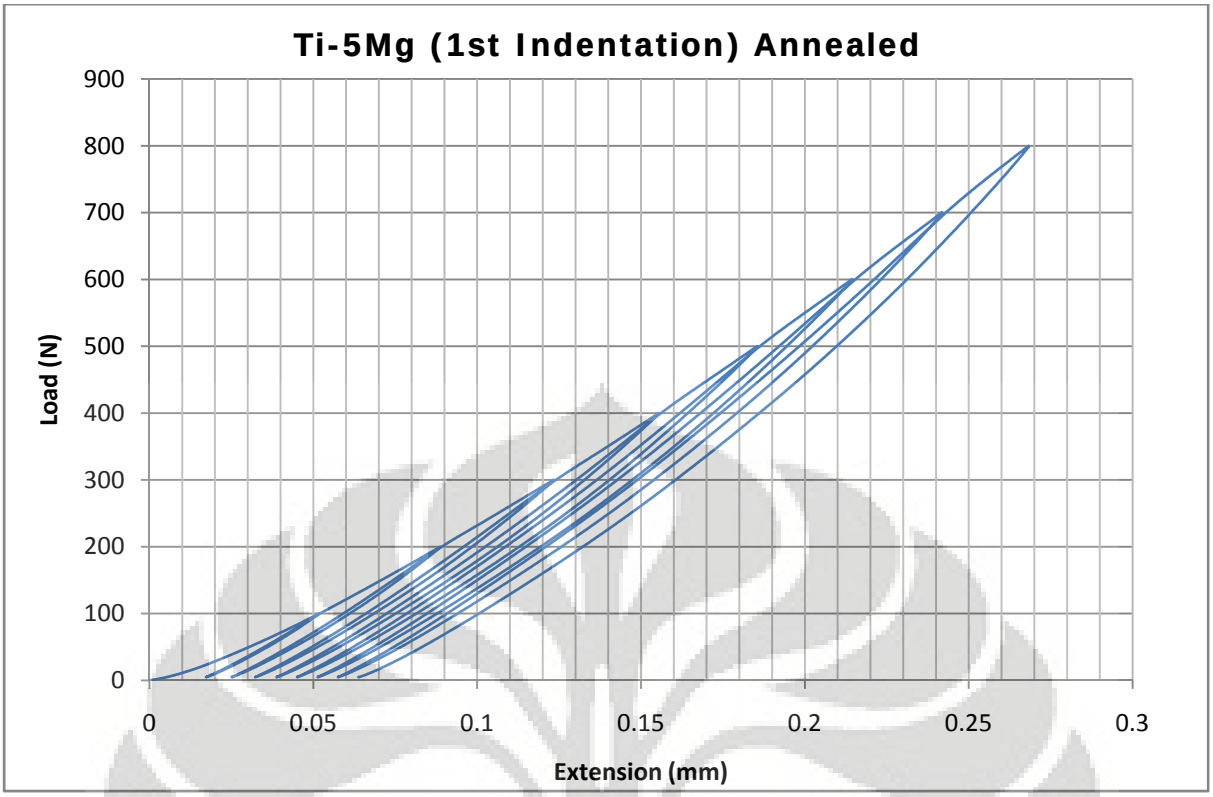
Ti-5Mg (1st Indentation) Annealed
Load (N)
900
800
700
600
500
400
300
200
100
0
0
0.05
0.1
0.15
0.2
0.25
0.3
Extension (mm)

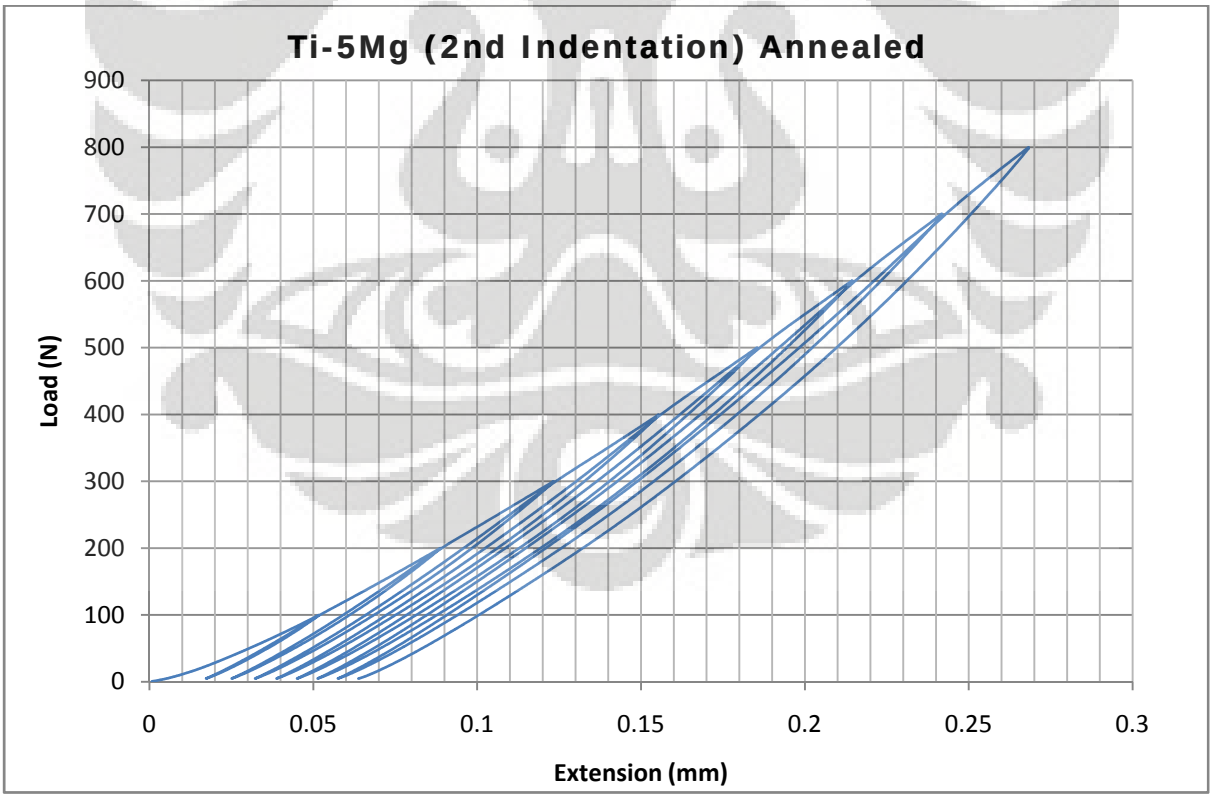
Ti-5Mg (2nd Indentation) Annealed
Load (N)
900
800
700
600
500
400
300
200
100
0
0
0.05
0.1
0.15
0.2
0.25
0.3
Extension (mm)

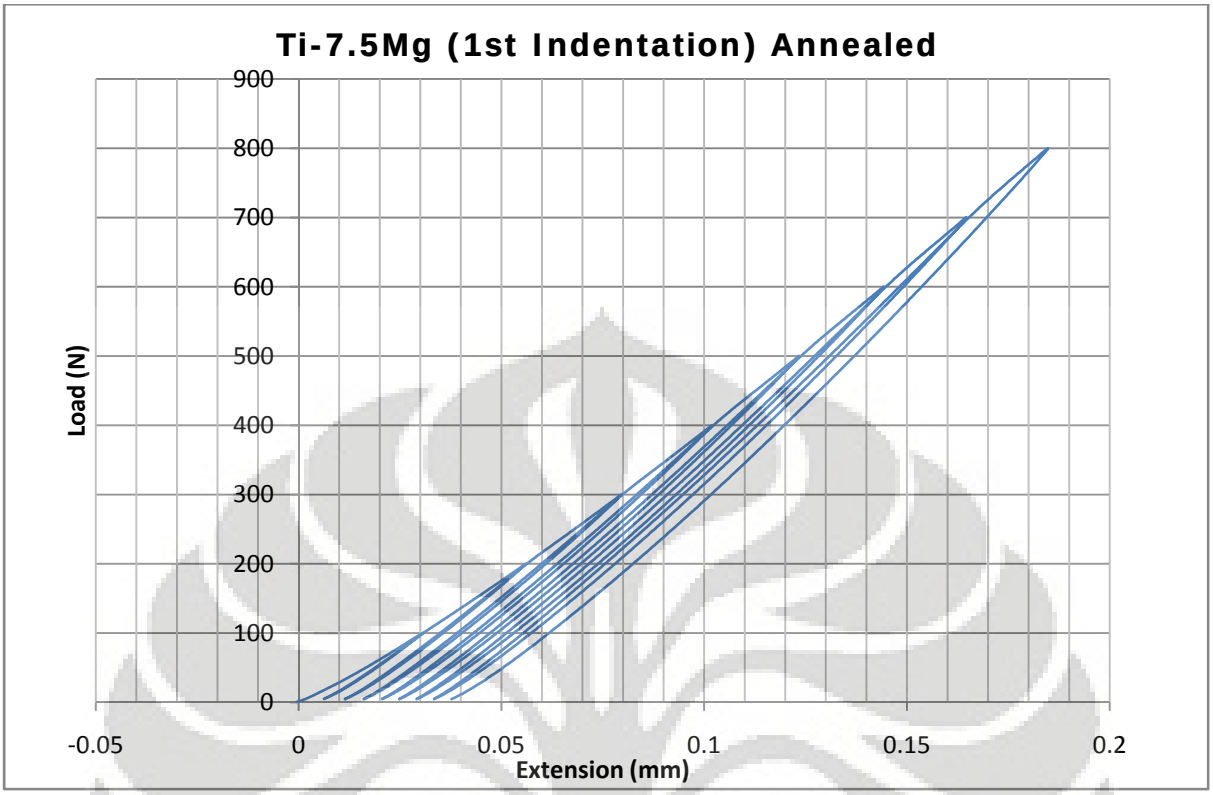
Ti-7.5Mg (1st Indentation) Annealed
Load (N)
900
800
700
600
500
400
300
200
100
0
-0.05
0
0.05
0.1
0.15
0.2
Extension (mm)

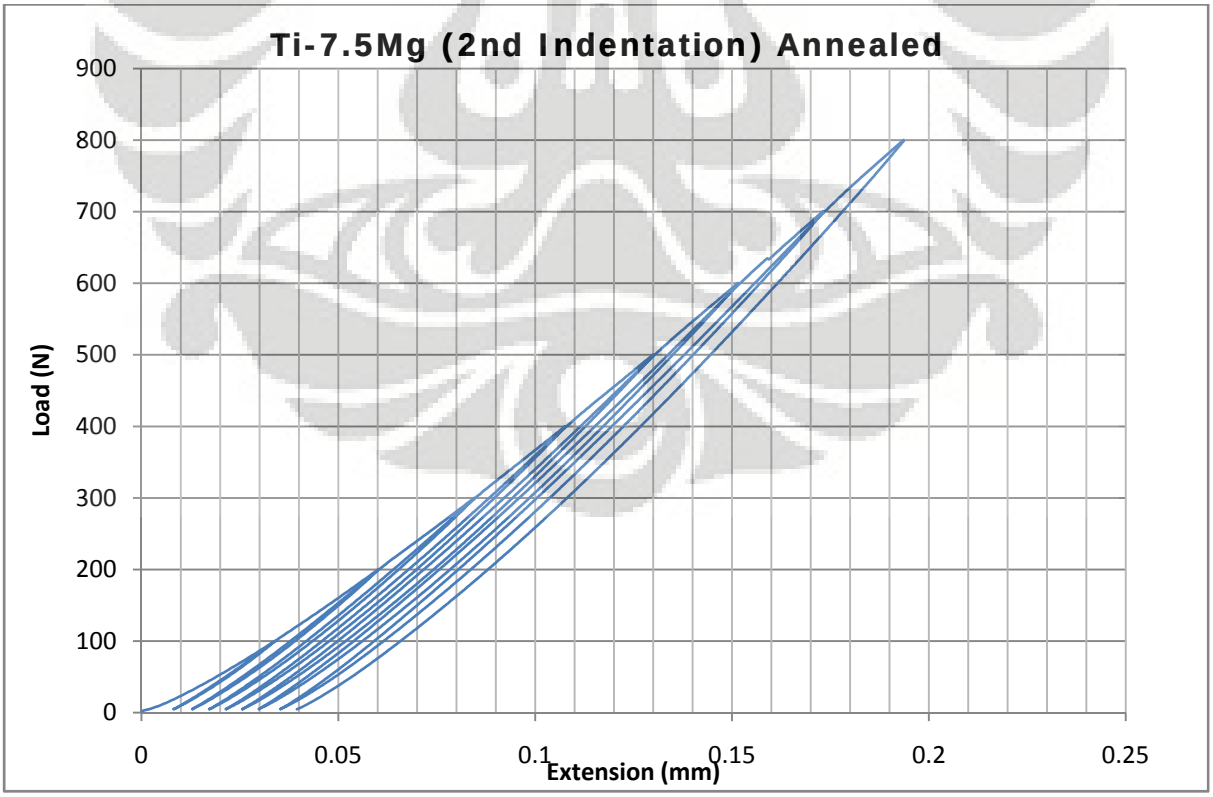
Ti-7.5Mg (2nd Indentation) Annealed
Load (N)
900
800
700
600
500
400
300
200
100
0
0
0.05
0.1
0.15
0.2
0.25
Extension (mm)

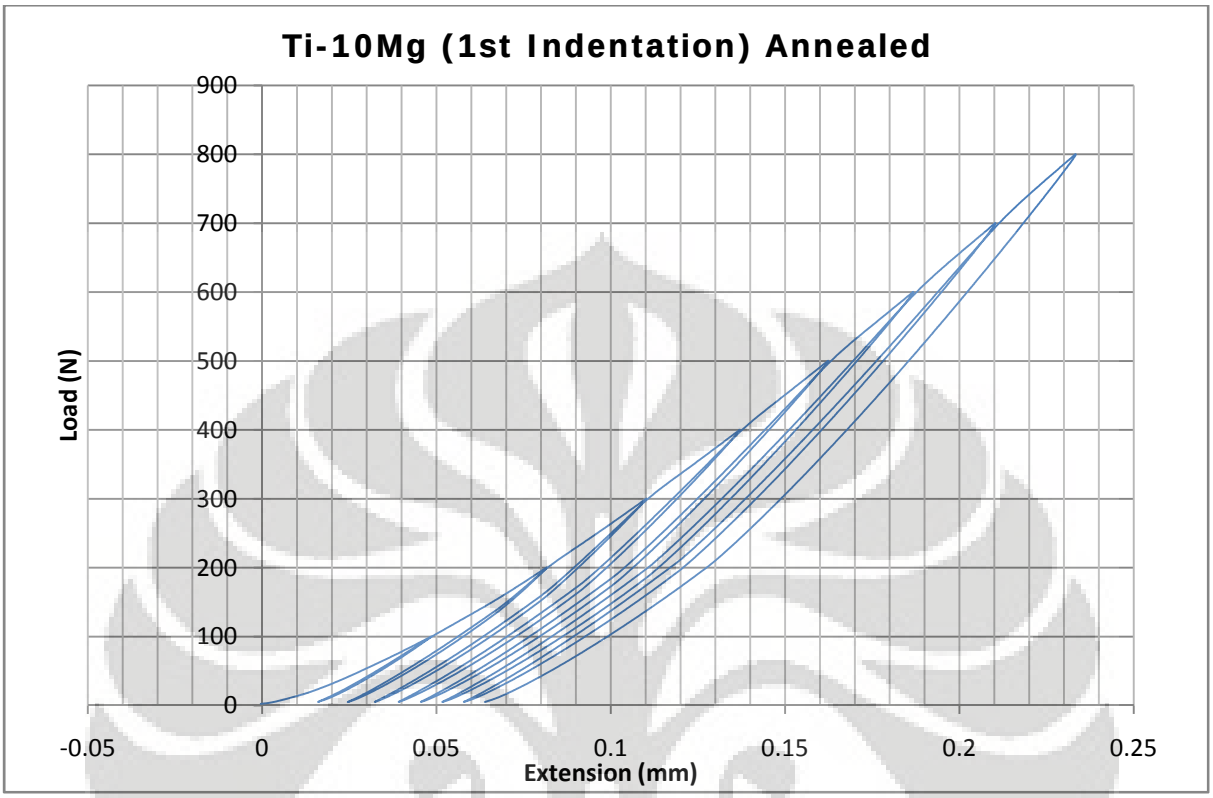
Ti-10Mg (1st Indentation) Annealed
Load (N)
900
800
700
600
500
400
300
200
100
0
-0.05
0
0.05
0.1
0.15
0.2
0.25
Extension (mm)

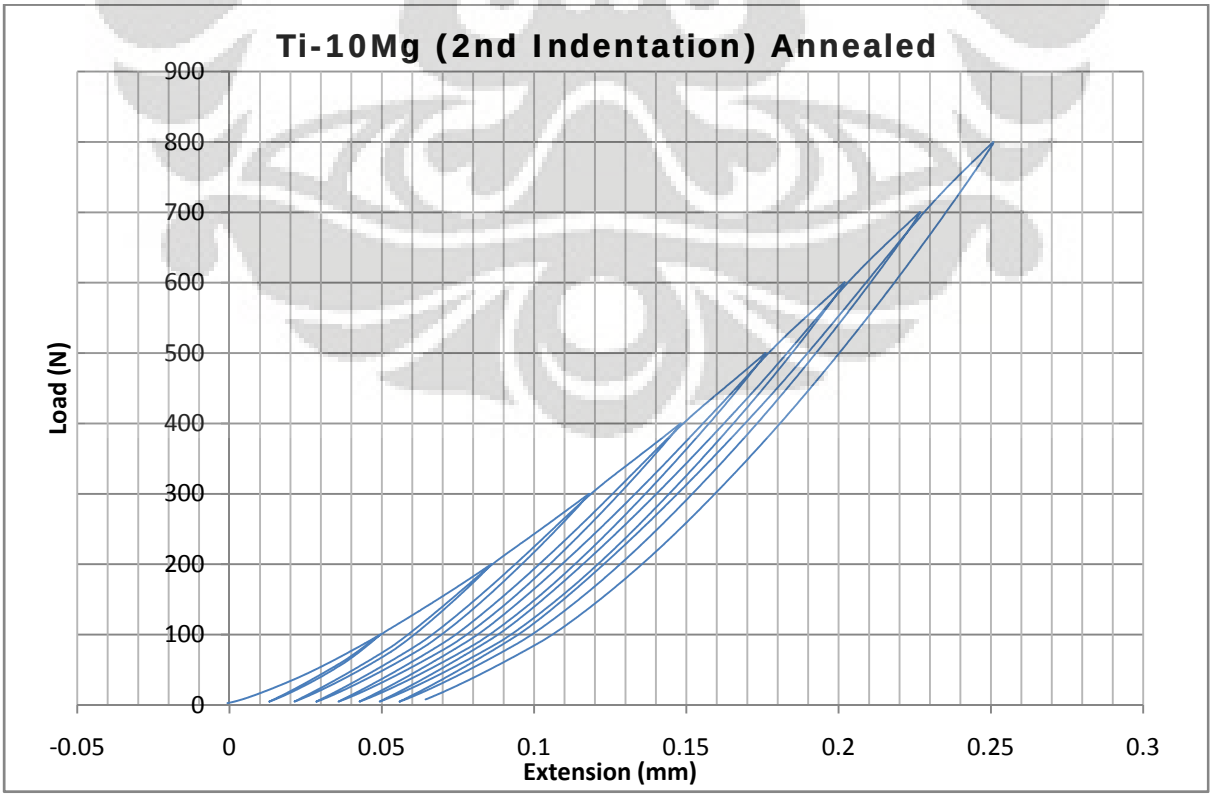
Ti-10Mg (2nd Indentation) Annealed
Load (N)
900
800
700
600
500
400
300
200
100
0
-0.05
0
0.05
0.1
0.15
0.2
0.25
0.3
Extension (mm)

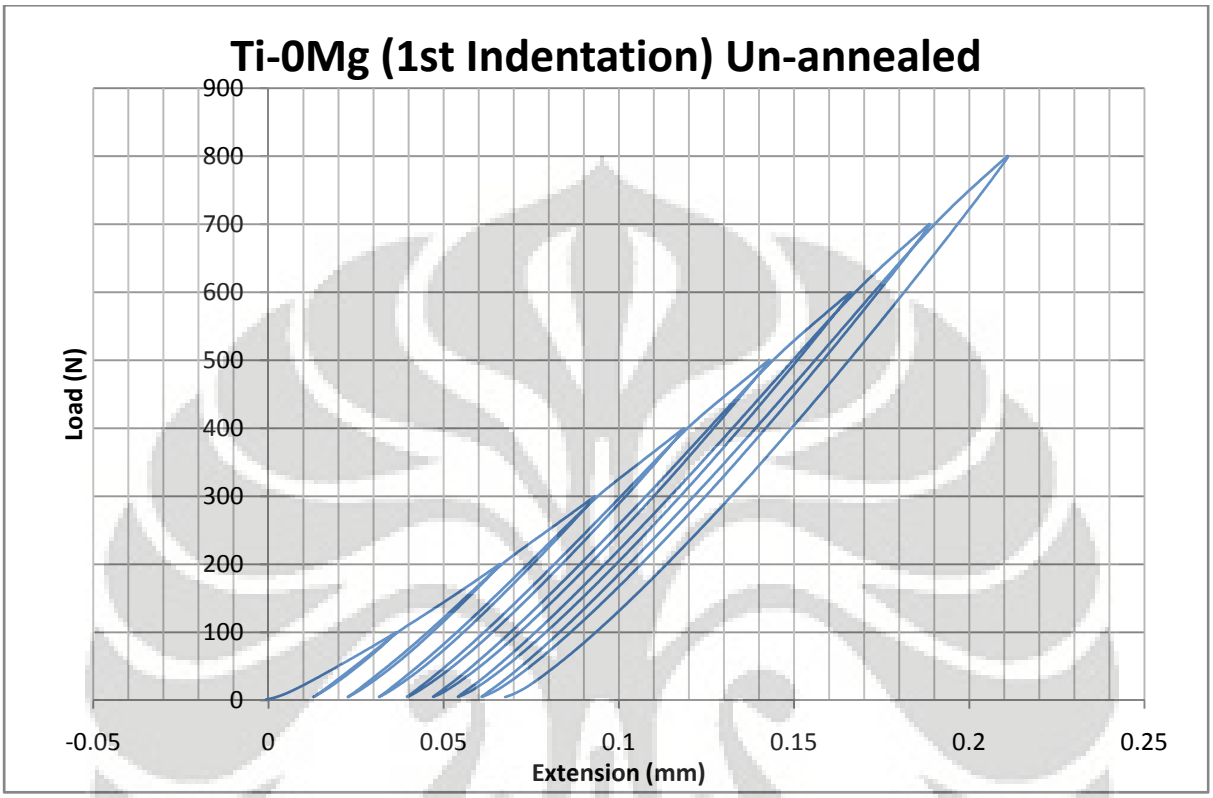
Ti-0Mg (1st Indentation) Un-annealed
Load (N)
900
800
700
600
500
400
300
200
100
0
-0.05
0
0.05
0.1
0.15
0.2
0.25
Extension (mm)

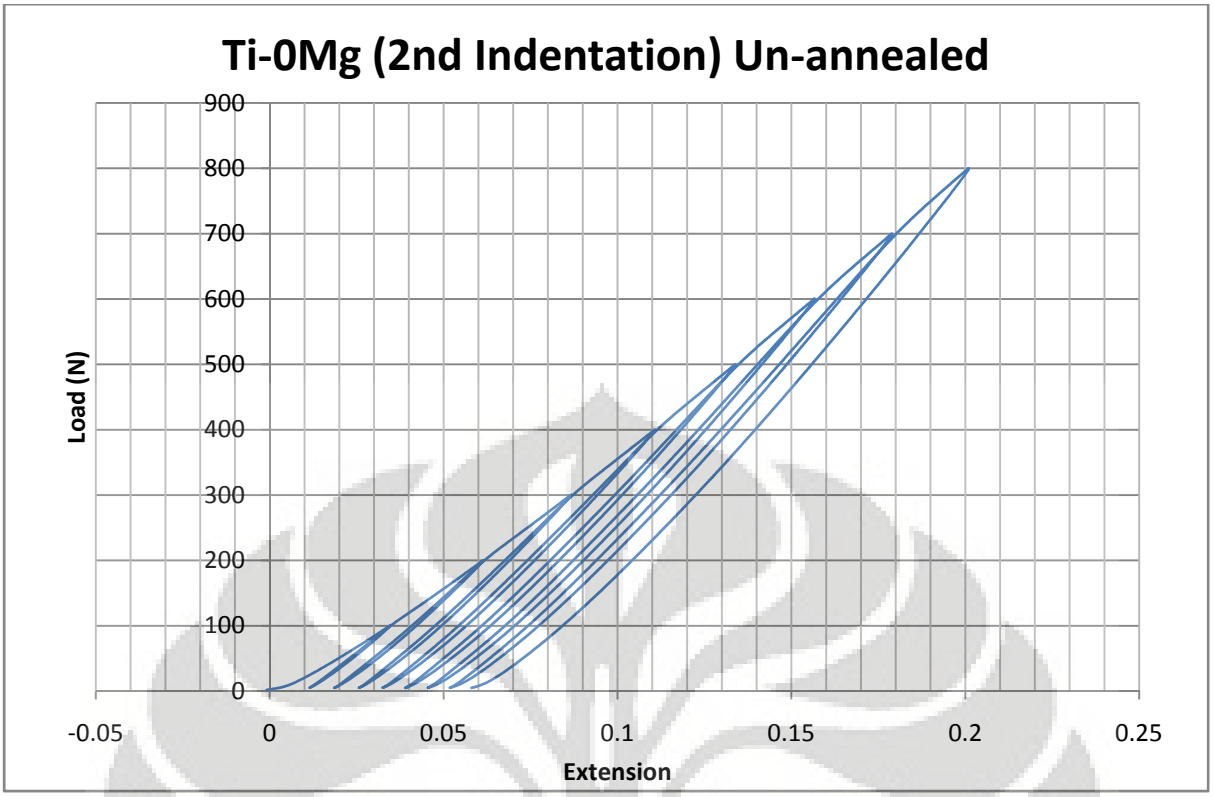
Ti-0Mg (2nd Indentation) Un-annealed
Load (N)
900
800
700
600
500
400
300
200
100
0
-0.05
0
0.05
0.1
0.15
0.2
0.25
Extension

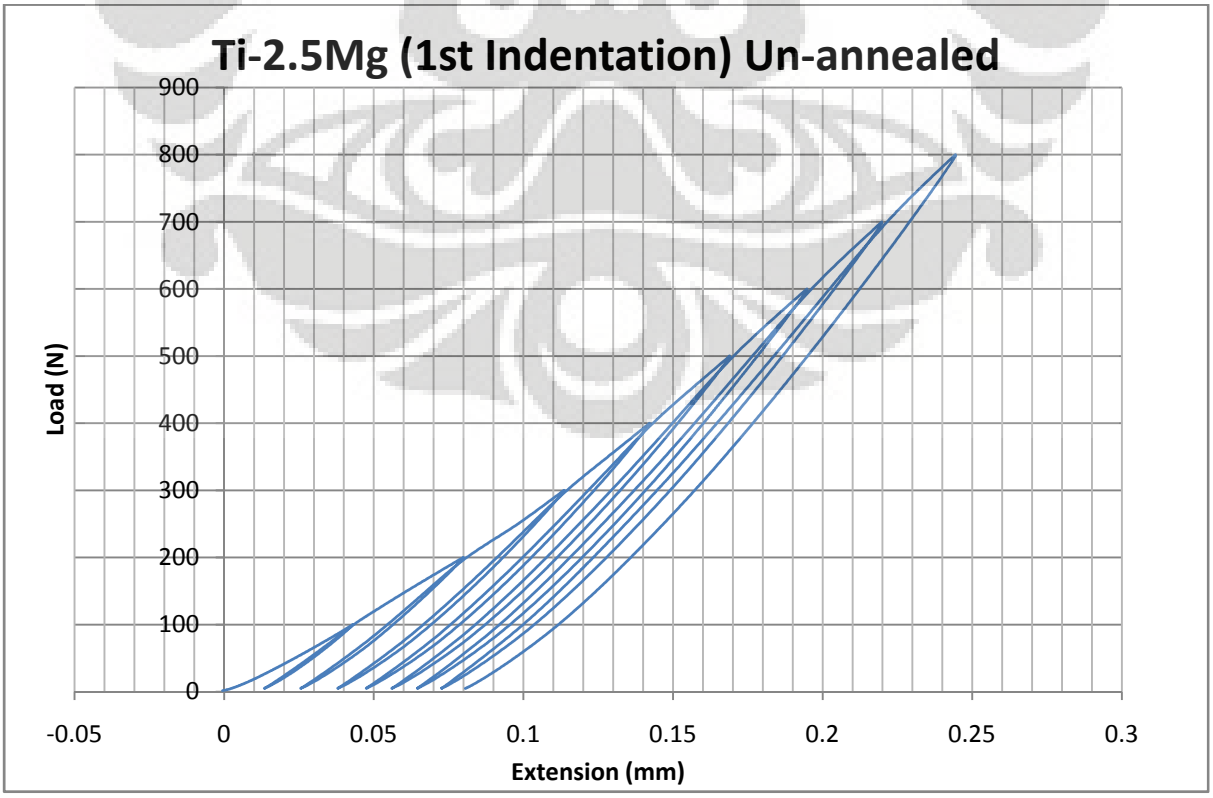
Ti-2.5Mg (1st Indentation) Un-annealed
Load (N)
900
800
700
600
500
400
300
200
100
0
-0.05
0
0.05
0.1
0.15
0.2
0.25
0.3
Extension (mm)

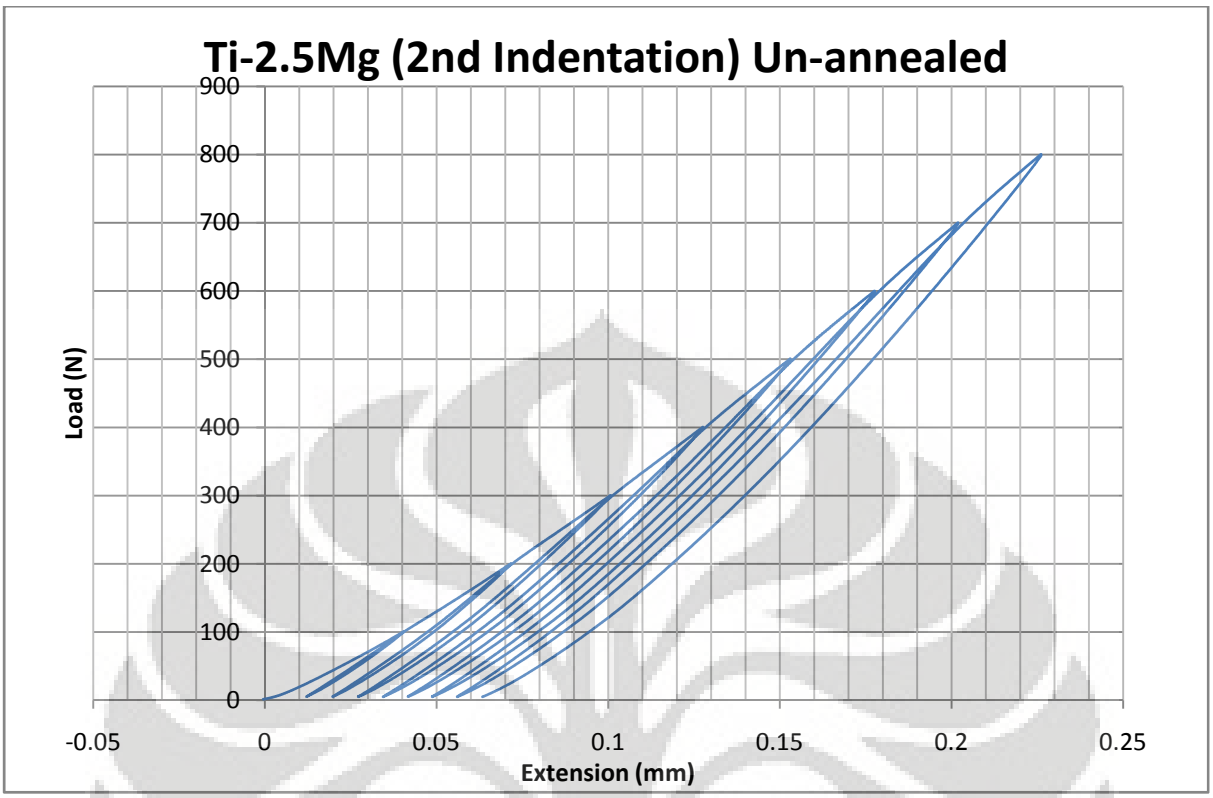
Ti-2.5Mg (2nd Indentation) Un-annealed
Load (N)
900
800
700
600
500
400
300
200
100
0
-0.05
0
0.05
0.1
0.15
0.2
0.25
Extension (mm)

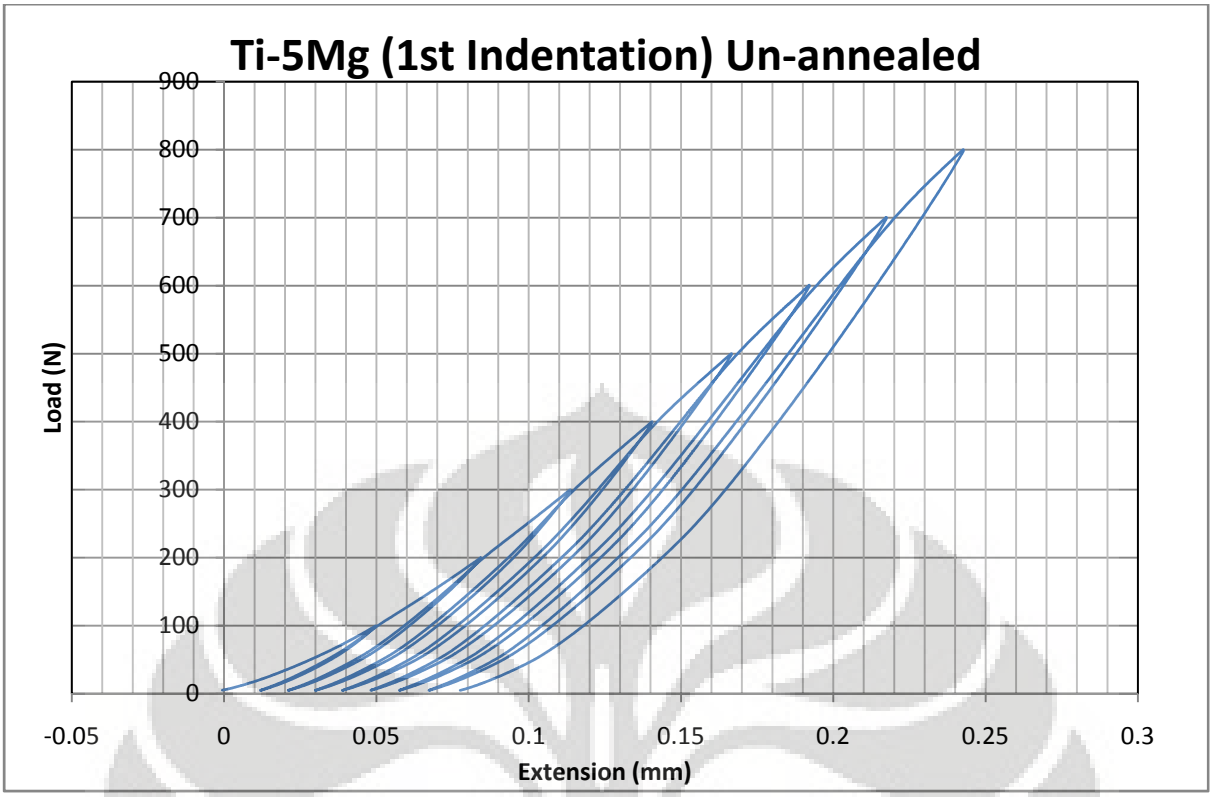
Ti-5Mg (1st Indentation) Un-annealed
Load (N)
900
800
700
600
500
400
300
200
100
0
-0.05
0
0.05
0.1
0.15
0.2
0.25
0.3
Extension (mm)

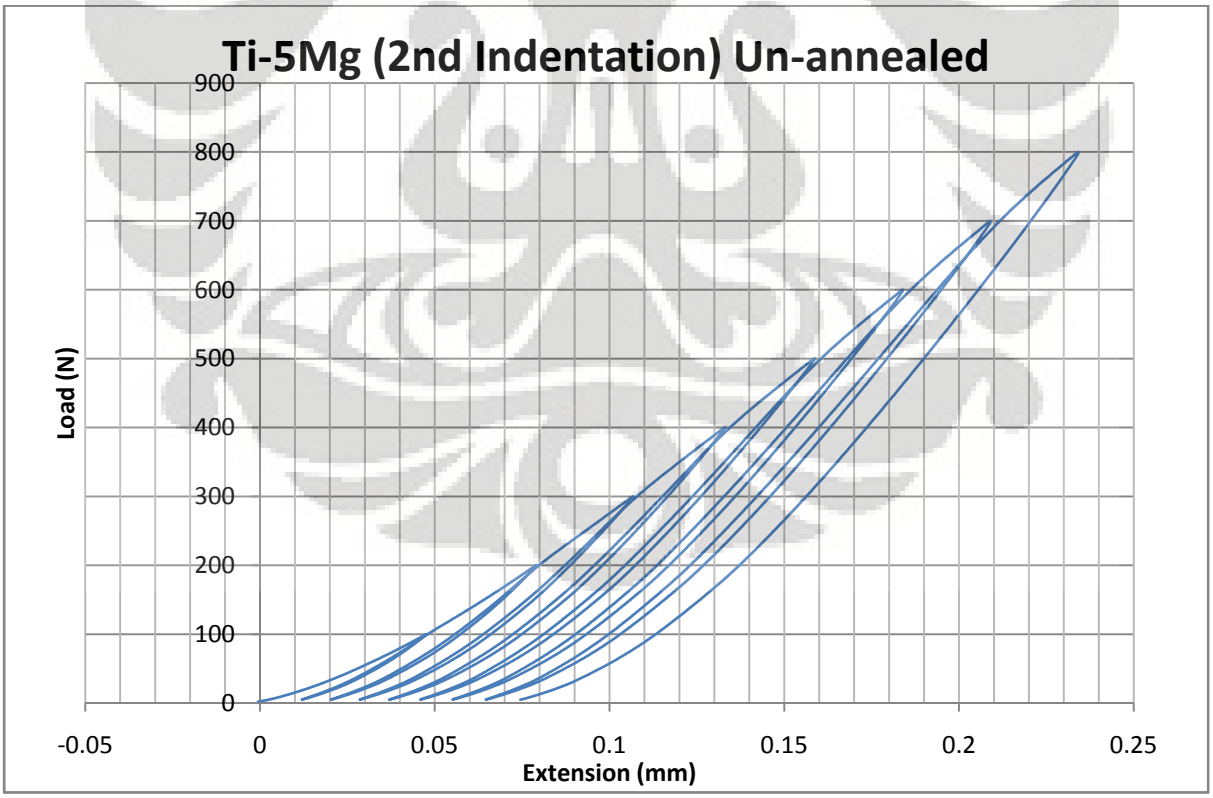
Ti-5Mg (2nd Indentation) Un-annealed
Load (N)
900
800
700
600
500
400
300
200
100
0
-0.05
0
0.05
0.1
0.15
0.2
0.25
Extension (mm)

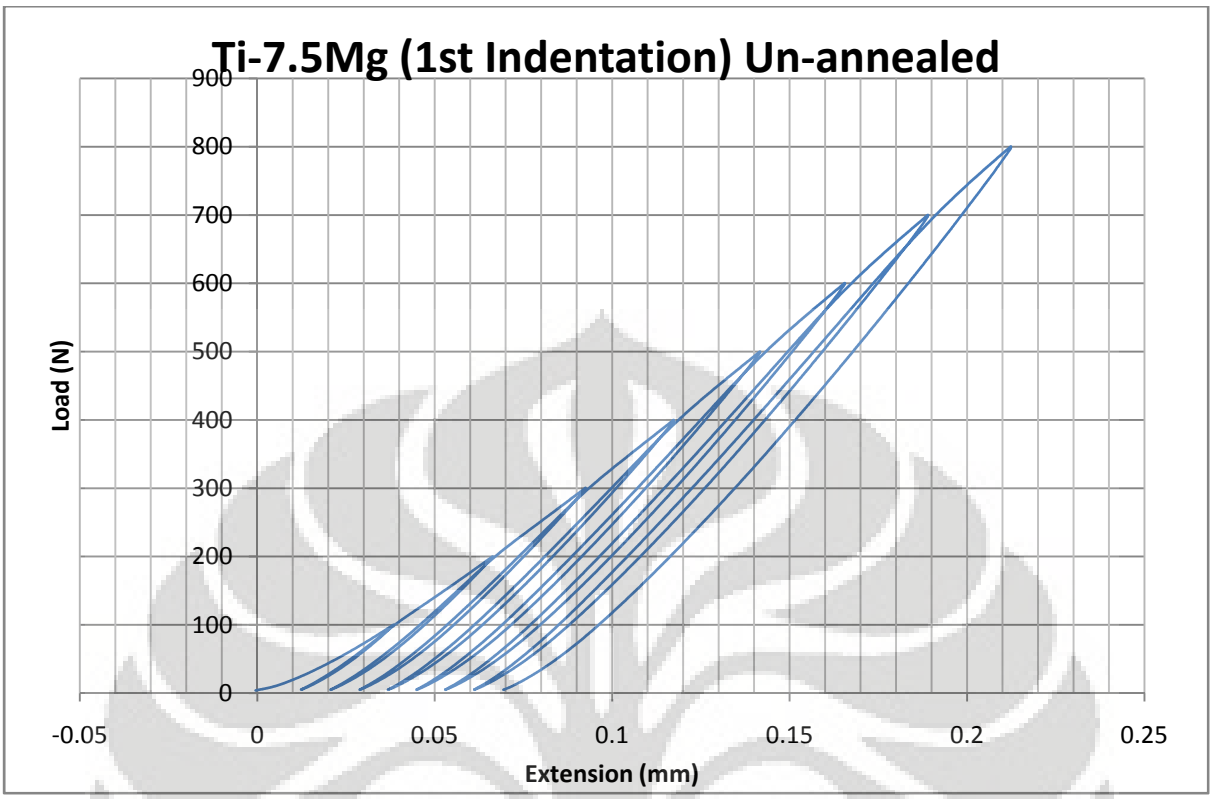
Ti-7.5Mg (1st Indentation) Un-annealed
Load (N)
900
800
700
600
500
400
300
200
100
0
-0.05
0
0.05
0.1
0.15
0.2
0.25
Extension (mm)

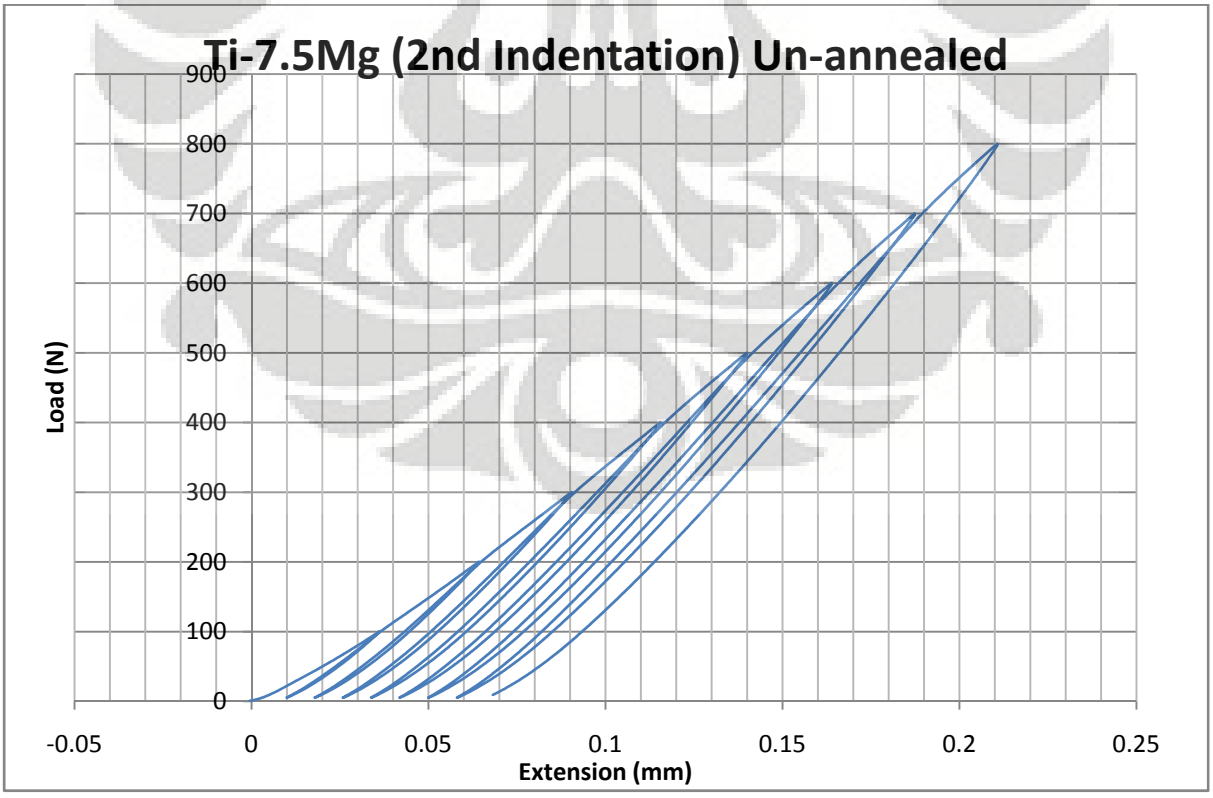
Ti-7.5Mg (2nd Indentation) Un-annealed
Load (N)
900
800
700
600
500
400
300
200
100
0
-0.05
0
0.05
0.1
0.15
0.2
0.25
Extension (mm)

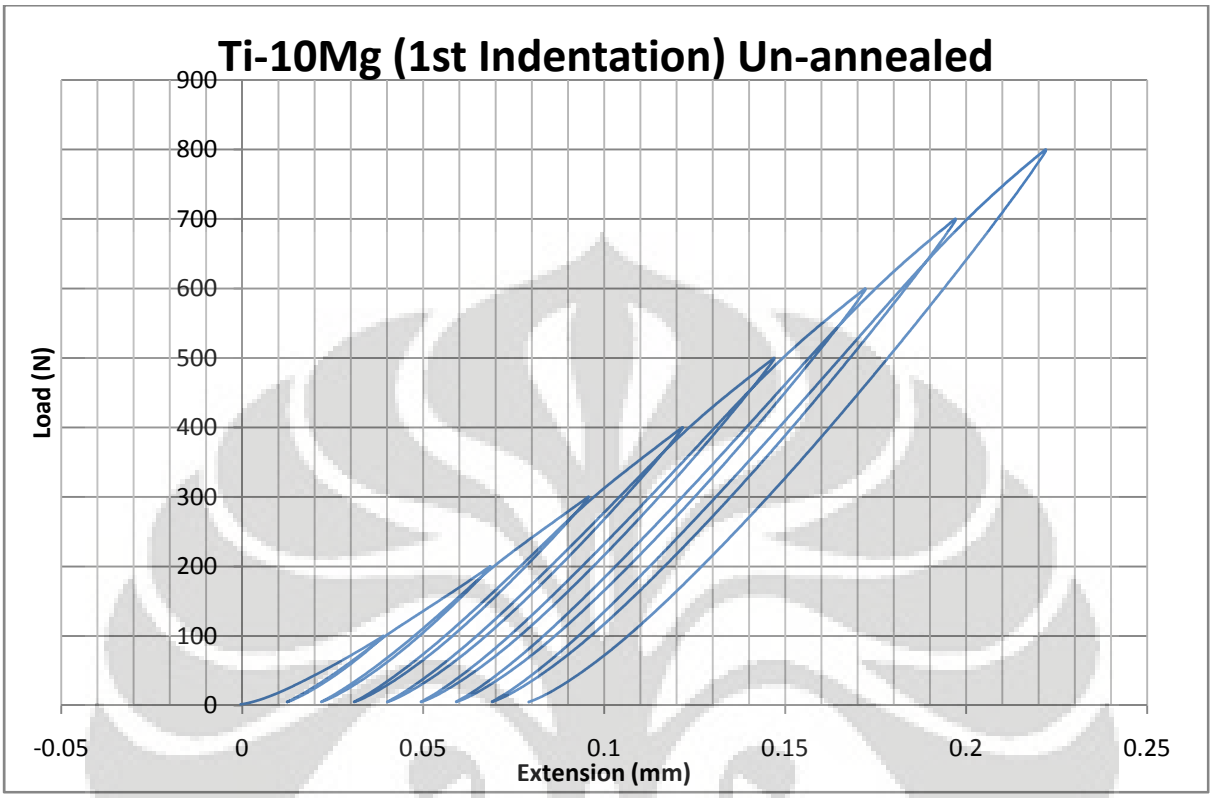
Ti-10Mg (1st Indentation) Un-annealed
Load (N)
900
800
700
600
500
400
300
200
100
0
-0.05
0
0.05
0.1
0.15
0.2
0.25
Extension (mm)

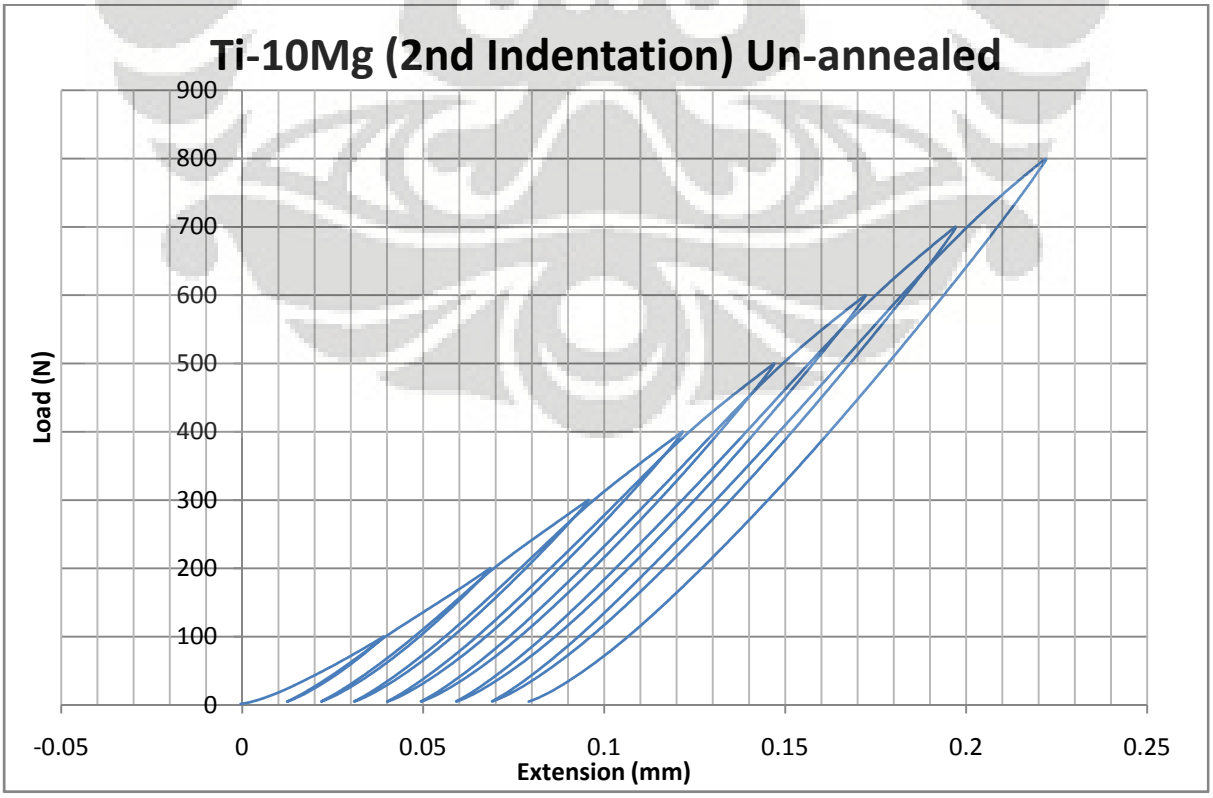
Ti-10Mg (2nd Indentation) Un-annealed
Load (N)
900
800
700
600
500
400
300
200
100
0
-0.05
0
0.05
0.1
0.15
0.2
0.25
Extension (mm)